Fall 2011

Investigation of the Impact of CO_2 on Water-Rock Interactions Using Sequential Extractions

Sarah Beers
San Jose State University

INVESTIGATION OF THE IMPACT OF CO_2 ON WATER-ROCK INTERACTIONS USING SEQUENTIAL EXTRACTIONS

A Thesis

Presented to

The Faculty of the Department of Geology

San José State University

In Partial Fulfillment

of the Requirements for the Degree

Master of Science

by

Sarah R. Beers

December 2011

The Dedicated Thesis Committee Approves the Thesis Titled

INVESTIGATION OF THE IMPACT OF CO_2 ON WATER-ROCK INTERACTIONS USING SEQUENTIAL EXTRACTIONS

by

Sarah R. Beers

APPROVED FOR THE DEPARTMENT OF GEOLOGY

SAN JOSÉ STATE UNIVERSITY

December 2011

Dr. June Oberdorfer	Department of Geology
Dr. David Andersen	Department of Geology
Dr. Yousif Kharaka	U.S. Geological Survey

ABSTRACT

INVESTIGATION OF THE IMPACT OF CO_2 ON WATER-ROCK INTERACTIONS USING SEQUENTIAL EXTRACTIONS

by Sarah R. Beers

Release of CO_2 into groundwater has an impact on groundwater geochemistry, including a decrease in pH, and increases in alkalinity and cation concentrations. From an experiment in Bozeman, Montana, it was concluded that the cations were released by interactions between groundwater, CO_2, and aquifer sediment. To evaluate these interactions, ions from the aquifer sediment were sequentially extracted to determine which cations and trace metals were associated with different phases in the sediment. These phases included ion exchange sites, carbonate, oxide, and sulfide minerals, and organic material. The data were then compared with the groundwater chemistry data to determine the likely reactions occurring in the aquifer with the addition of CO_2.

Geochemical groundwater modeling revealed that the groundwater was undersaturated with respect to calcite both before and during the addition of CO_2. Thus, calcite dissolution was contributing to the groundwater chemistry. In addition to calcite dissolution, a decrease in pH in the aquifer affected ion exchange and manganese oxide dissolution. Comparisons between the sequential extraction results and groundwater chemistry showed that uranium and barium were closely related to carbonate dissolution, while magnesium and strontium were primarily contributed by ion exchange. Also, manganese oxides contributed a majority of the cobalt in the system. Ion exchange, carbonate dissolution, and manganese oxide dissolution are responsible for a majority of the groundwater geochemical changes as a result of CO_2 injection.

ACKNOWLEDGEMENTS

First, my thanks go out to the faculty and staff of the Department of Geology at San Jose State University, especially my advisor Dr. June Oberdorfer who has helped me with my thesis and through my entire graduate career. I would like to thank my colleagues at the U.S. Geological Survey in Menlo Park, California, especially my supervisor and mentor Dr. Yousif Kharaka, for their guidance, support, and knowledge that helped me to finish my thesis project. I have enjoyed the short time that I have spent working with you. I would also like to thank my loving husband for his support and encouragement over the years; I am so happy you are a part of my life. Finally, I extend my gratitude to my parents for always encouraging me to continue my education, and my friends for sharing the excitement each time I reached a thesis milestone. I am truly lucky I have you as my colleagues, family, and friends.

TABLE OF CONTENTS

LIST OF FIGURES

Figure

LIST OF TABLES

Table

INTRODUCTION

Greenhouse gas emissions and their contribution to global warming are a growing concern in environmental science. The concentration of carbon dioxide, one of the major greenhouse gases, has been rising steadily in the atmosphere, which has led to increased global temperatures and increased ocean acidification (Intergovernmental Panel on Climate Change (IPCC), 2005). One option to mitigate impacts of global warming is to reduce carbon dioxide emissions by carbon capture and sequestration (CCS). CCS is a proposal to collect carbon dioxide from fuel-burning plants and inject it deep underground into saline aquifers or depleted oil reservoirs (IPCC, 2005). Underground storage has prompted many groups to study possible impacts of CO_2 leaks into the near-surface environment.

The Zero Emissions Research and Technology (ZERT) group, led by Lee Spangler of Montana State University (MSU) in Bozeman, Montana, is a multi-disciplinary group of scientists who are developing tools to monitor and detect shallow and near-surface changes as a result of a carbon dioxide leak associated with geologic carbon sequestration (GCS) (Spangler et al., 2009). To simulate a leak of sequestered carbon dioxide, gaseous carbon dioxide was introduced into a shallow aquifer using a buried, horizontal, perforated pipe. The addition of CO_2 resulted in changes in groundwater chemistry, including a decrease in pH (7.0 to 5.6), and increases in alkalinity (400 to 1,330 mg/L as HCO_3) and in concentrations of major and minor cations and trace metals (Kharaka et al., 2010). Many of these trace metals, including chromium,

copper, lead, and uranium, are harmful to human health, and their concentrations in drinking water are regulated by the U.S. Environmental Protection Agency (U.S. EPA). Integral to understanding the sources of these metals is determining the water-mineral interactions following CO_2 injection.

The goal of this research is to identify the minerals and the physio-chemical processes responsible for the observed changes in the chemical composition of groundwater following CO_2 injection. To achieve this, sediment from the CO_2-injection site was subjected to sequential extractions, using a series of increasingly stronger chemical reagents, in an effort to determine the concentrations of metals participating in exchangeable reactions and those released by dissolution of carbonate, hydrous oxide, crystalline oxide, and silicate minerals.

BACKGROUND

The ZERT Project

CCS is a rapidly-growing field associated with concern over increasing concentrations of CO_2 in Earth's atmosphere. The IPCC notes that carbon capture and sequestration is one way to immediately reduce the amount of CO_2 released into the atmosphere; however, there are many remaining facets of the technology, including the environmental impact, that are understudied (Holloway, 2005; IPCC, 2005). The U.S. Geological Survey (USGS) is investigating methods to detect geochemical changes resulting from injecting CO_2 into a shallow, freshwater aquifer at the ZERT experimental site in Bozeman, Montana (figures 1 and 2). The ZERT experimental site is in a MSU agricultural field, approximately 2 km west of the main campus. The ZERT project will aid in creating near-surface monitoring and detection technologies directed at identifying CO_2 leaks into shallow, subsurface aquifers from GCS sites.

For one month during the summers of 2008 and 2009 at the ZERT experimental site, 300 kg/day and 200 kg/day, respectively, of CO_2 were injected into a horizontal, perforated pipeline. The pipeline is situated 2 to 2.3 m beneath the ground surface, at a depth approximately 1 m below the water table (Spangler et al., 2009; Kharaka et al., 2010). Before and during the injection, water samples were regularly collected from ten monitoring wells (Figure 2). Kharaka et al. (2010) reported rapid changes in pH, alkalinity, and electrical conductivity of the groundwater associated with the CO_2

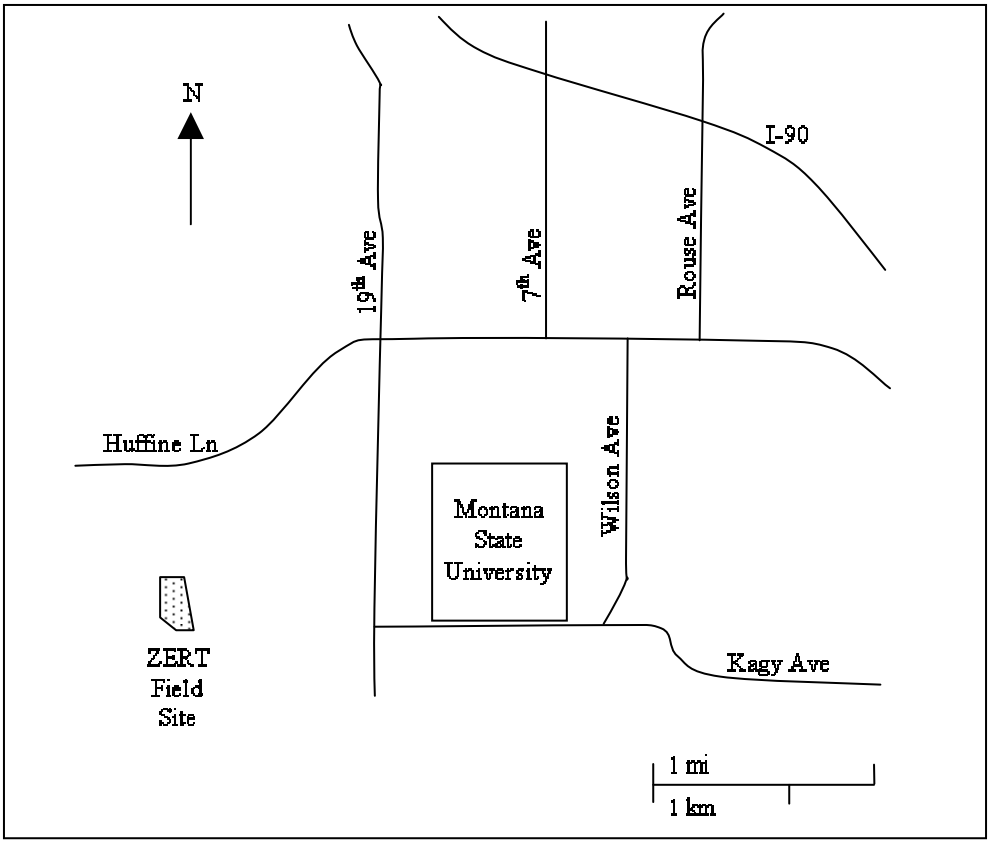

Figure 1. Location of the ZERT experimental site in Bozeman, Montana. The experimental site is approximately 2 km west of Montana State University.

injection (2008 data published in Kharaka et al., 2010; 2009 data unpublished). Increases were shown for alkalinity (400 to 1,330 mg/L as HCO_3) and electrical conductance (700 to 1,800 μS/cm), while pH decreased (7.0 to 5.6).

The decrease in pH is reasonable because CO_2 converts to carbonic acid, thus lowering the pH of the groundwater (Kharaka et al., 2010). In response to lowered pH, carbonate minerals should dissolve more readily, thus raising alkalinity and electrical conductance of the groundwater (Kharaka et al., 2010). Furthermore, the addition of CO_2 to groundwater increases the mobility of some cations, including calcium, magnesium,

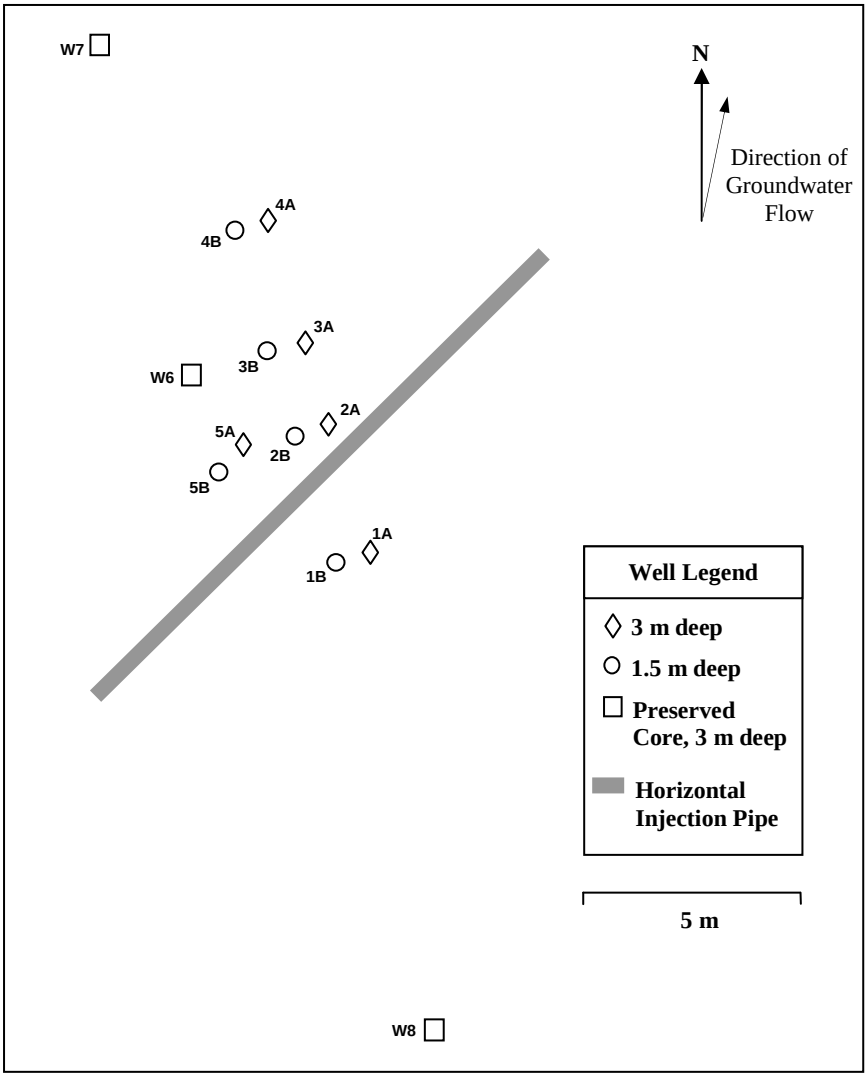

Figure 2. Map of the ZERT water monitoring site (modified from Kharaka et al., 2010). W6, W7, and W8 are 3 m deep, and their respective cores were saved for logging and for sequential extractions.

iron, and chromium, which is evidenced by increased concentrations in the groundwater from levels measured before the injection (Kharaka et al., 2010). Mobilization of some metals is of concern due to the adverse health effects they may cause to biota, including humans.

The U.S. EPA regulates the concentrations of some metals in human drinking water. A list of EPA's drinking water standards for relevant metals and common health effects can be found in Table 1. Potentially toxic elements that showed increases in concentrations during the CO_2 injection at ZERT include barium, cadmium, chromium, copper, iron, manganese, lead, uranium, and zinc (Kharaka et al., 2010). Six of these elements have primary restrictions in drinking water instituted by the EPA.

Table 1. U.S. EPA primary drinking water standards for selected elements. Included are allowed maximum contaminant levels (MCL), and long-term exposure health effects caused by those elements (modified from U.S. EPA, 2009).

	MCL (mg/L)	**Potential Health Effects from Long-Term Exposure above the MCL**
Inorganic Chemicals		
Barium (Ba)	2.00	- Increase in blood pressure
Cadmium (Cd)	0.005	- Kidney damage
Chromium (Cr)	0.10	- Allergic dermatitis
Copper (Cu)	1.30	- Gastrointestinal disease - Liver or kidney damage
Lead (Pb)	0.015	- Delays development in infants and children - Kidney problems and high blood pressure in adults
Radionuclides		
Uranium (U)	0.03	- Increased risk of cancer - Kidney toxicity

The sources and species of these elements in ZERT groundwater are discussed below, however it is hypothesized that a majority of the elements are mobilized from ion-

exchange and carbonate dissolution resulting from the decreased pH caused by CO_2 injection (Kharaka et al., 2010).

Geology

Regional Geology

Bozeman, Montana, is in the eastern Gallatin Valley situated at the foot of the Gallatin Mountains to the south and the Bridger Mountains to the east. The streams and rivers are dominated by flows from the Gallatin Mountains, which also provide much of the sediment filling the eastern part of the valley. Outcrops in the Gallatin Mountains include Achaean metamorphic rocks at the base of the mountain, overlain by Paleozoic rocks such as the Madison Formation and other marine sedimentary rocks, and topped by Absaroka volcanic rocks deposited in the Cenozoic.

Bozeman sits on what is informally called the "Bozeman Fan." Two conflicting theories for the origin of this fan were published by Montana Bureau of Mines and Geology in 2002. Older research claims the Bozeman Fan consists of alluvial sediment from two units (Vuke et al., 2002). The older unit, being Tertiary in age, is composed of conglomerate, sandstone, siltstone, and volcanic ash beds, and is up to 360 m (1,200 ft) thick. Overlying this is a younger Quaternary unit, approximately 240 m (800 ft) thick and alluvial in origin, that consists of bouldery gravel with some sand and silt. The gravel clasts consist of Precambrian metamorphic clasts, mafic volcanic rocks, dacite, sandstone, and limestone (Vuke et al., 2002).

The opposing research also suggests two units underlying the Bozeman Fan (Lonn and English, 2002). The older unit, called the Sixmile Creek Formation, is very thick and consists of Tertiary sediment that is very fine grained with interbedded tuffaceous siltstone. Overlying this is a very thin (30 ft) gravel deposit thought to be the result of glacial outwash in the Pleistocene (Lonn and English, 2002). These two units together create a shallow, perched aquifer under Bozeman and the surrounding area (Lonn and English, 2002). Lonn and English (2002) based their research on core logs from the area.

Site Geology

In December 2008, three new wells were drilled at the ZERT site and the resulting cores were preserved for sediment analysis, including sequential extractions. The sediment analyzed was sampled from three, 3 m-deep cores shown as W6, W7, and W8 in Figure 2. Each core exhibits an organic, clay-rich A horizon (26 to 45 cm thick), a fine-grained carbonate-rich B horizon (23 to 44 cm thick), and coarse, sandy gravel extending through the rest of the core. Core logs can be found in Appendix A. The sediment is poorly sorted, and the composition is very heterogeneous. Common among the gravel and sand are clasts of dacite, granite, basalt, gneiss, and limestone. In addition, the sandy gravel is rich in magnetite and secondary carbonate.

The aquifer beneath the ZERT site is considered a drinking water aquifer, and it resides in the upper Quaternary sediment described above. It contains fresh water with background total dissolved solids of 570 mg/L, low alkalinity of about 400 mg/L as

HCO_3^-, and low concentrations of dissolved nitrate and sulfate (Kharaka et al., 2010). During the summer months, the water table is located approximately 1 m below the ground surface in the sandy-gravel sediment. Groundwater monitoring revealed that the local groundwater gradient is approximately N11E. A tracer test indicated a pore velocity of approximately 3 m/day, and a pumping test resulted in a horizontal hydraulic conductivity of 24 m/day. Finally, core testing indicates a porosity of 23-28% in the sandy gravel (unpublished data).

Sequential Extraction Procedures

Scientists have been using sequential extractions for decades to evaluate elemental constituents in soils related to plant bioavailability, mineral prospecting, and environmental contamination (Papp et al., 1991; Modak et al., 1992; Hall et al., 1996). It has been determined that the reagents and concentrations selected for sequential extraction procedures are dependent on the mineral phases in the sediment. The results obtained are "operationally defined," meaning selective dissolution of only one phase is difficult, and the experimental results are sensitive to reagent choice, sediment to reagent ratio, and reaction times (Tessier et al., 1979; Hall et al., 1996; Kennedy et al., 1997). However, relationships emerge with repeated extractions; these in conjunction with water quality results from the CO_2 injection at the ZERT site can be used to infer the physio-chemical changes responsible for the release of metals into the groundwater.

METHODS

Core Sampling

ZERT sediment cores were collected in December 2008, approximately four months after a CO_2-injection period at the ZERT field site. Figure 2 shows a map of the well field at the ZERT site. W8 is approximately 11 m upgradient from the horizontal CO_2 injection pipe; therefore, it is assumed this core was unaffected by CO_2. W6 lies within the well field approximately 4 m downgradient from the horizontal CO_2 injection pipe, and it is likely that the sediment from this core has been affected by the experiment. W7 is located approximately 10 m downgradient from the horizontal injection well, and changes in groundwater quality due to CO_2 injection were not observed in this well. Due to their greater distance from the injection pipe, sediment from W7 and W8 was analyzed for this experiment. A diagram of the samples collected from W7 and W8 is shown in Figure 3.

The sediment from each well core that was extracted included one sample from each well of the following soil types: 1) A horizon clay-rich sediment (Topsoil), 2) B horizon carbonate-rich sediment, 3) sandy-gravel sediment near the water table (denoted SSG in the results), and 4) sandy-gravel sediment from the bottom of the cores (DSG). In addition, two duplicate aliquots from the carbonate-rich B horizon and the sandy gravel section in W8 were analyzed for quality control of the experiment. These two samples were specifically chosen because B horizon sediment and SSG sediment are likely the

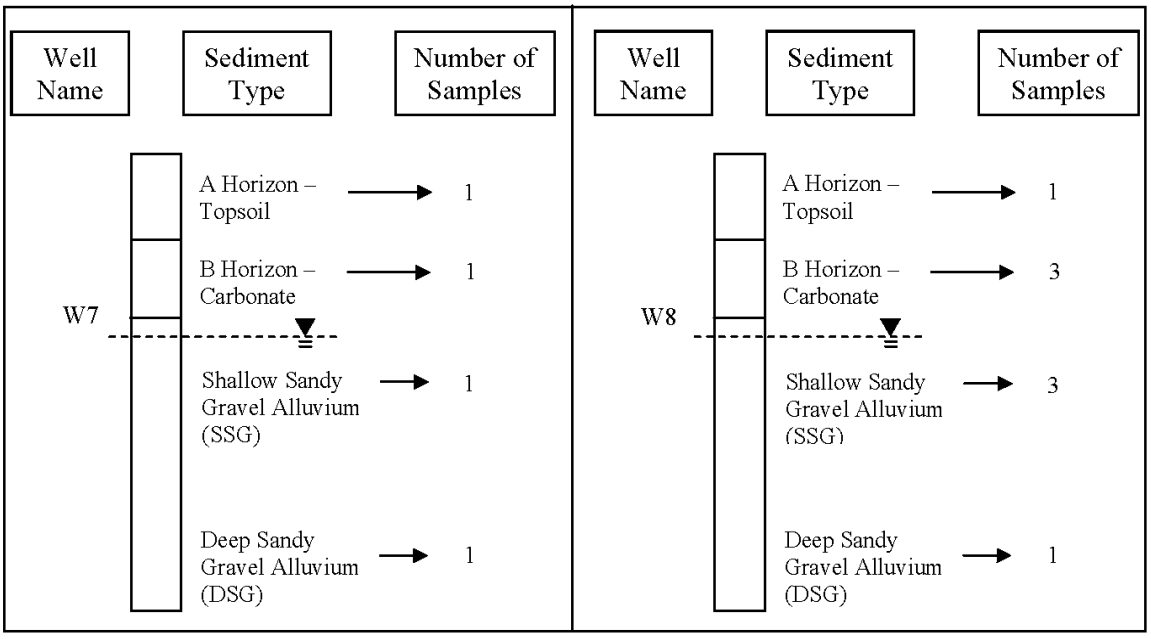

Figure 3. Samples selected for sequential extractions. The water table is denoted by the dashed line and inverted triangle. Note: not drawn to scale.

most affected by interactions with CO_2; also, these two core subsamples had ample amounts of sediment available for extractions. In total, 12 sediment samples underwent the sequential extraction.

Sample Preparation

A series of sediment samples was taken from the cores from W7 and W8 for analysis. All samples were air dried and sieved; the sequential extractions were performed on sediment that passed a 2.0 mm mesh sieve, equivalent to grains that are sand-sized and smaller. This fraction was selected because a majority of the water-rock

interactions occur at grain surfaces (Krauskopf and Bird, 1995). Due to the high surface area to volume ratio, smaller grains are considered more reactive than larger grains. After sieving to < 2.0 mm, the sediment was homogenized by mixing and split into 5.0 g aliquots using a riffle splitter, in accordance with EPA Method 823B (U.S. EPA, 2001). Five-gram samples are large compared to those used by other researchers (Tessier et al., 1979; Hall, 1998). However, larger samples were needed in this experiment because the sandy gravel is highly heterogeneous. A minimum of 5.3 grams is suggested for sediment sieved to < 2.0 mm, but a compromise had to be made to accommodate reagent volumes, and available laboratory space and equipment (Jackson, 1958). The 5.0 g sediment aliquots were transferred to acid-washed, 50 mL polypropylene centrifuge tubes for the sequential extraction. Remaining sediment was visually characterized using a reflected-light microscope to identify major components of the sediment.

Before the experiment, all glassware, plasticware, and utensils were acid washed to ensure they were free from metal contamination. After each extraction, the reagent-sediment slurries were centrifuged, and the supernatant was decanted, filtered to < 0.1 μm, acidified with HNO_3 when necessary, and stored in acid-washed polypropylene bottles until analysis.

Sequential Extraction Reagents

Sequential extractions use a series of reagents that typically increase in reactive strength and decrease in pH in order to selectively dissolve minerals. Reagents and

procedures vary depending on the minerals present in the sediment of interest. ZERT aquifer sediment contains clays and other particle surfaces that participate in ion exchange, as well as minerals such as carbonates, amorphous and crystalline oxides, sulfides, and organic matter. All of these have the potential to release cations into the groundwater with changing groundwater chemistry, as with the case of CO_2 injection. Thus, the reagents and procedures were chosen to selectively focus on ion exchange or dissolution of the listed minerals. The reagents and procedures used in this research are shown in Table 2. The sample to solution (volume/volume) ratio used for each extraction step was 1:10.

Ion Exchange

Sequential extractions generally begin with weak acid or salt solutions designed to displace exchangeable cations. This includes cations that are electrostatically bonded to grain surfaces, especially surfaces of clay minerals, or cations that are easily exchanged in crystal lattices (Krauskopf and Bird, 1995). Ion exchange is sensitive to the substrate, the pH of the surrounding solution, the cation composition of the surrounding solution, and many other properties. Clays such as the smectite and kaolinite that were identified in the ZERT sediment are important soil components for ion exchange because of the surface charges produced by the clay mineral structure (Krauskopf and Bird, 1995). The ZERT soil has high clay concentrations in the topsoil and B horizons, with many fewer clay-sized particles occurring in the sandy gravel.

Table 2. Sequential extraction procedures utilized.

Target	Reagent	Duration	Temperature	Agitation	Source
A - Ion Exchange	1.0M Cesium Chloride	30 mins, repeat once	25˚C	constant	Reardon et al., 1983
B - Carbonate	1.0 M sodium acetate - acetic acid buffer (pH=5)	5 hours	25˚C	constant	Tessier et al., 1979; Chao, 1984; Maher, 1984
C - Mn Oxides and Amorphous Oxides	0.25 M hydroxylamine hydrochloride in 0.25 M HCl	2 hours, repeat for 30 mins	60˚C	every 30 mins	Hall et al., 1996
D - Crystalline Fe Oxides	1.0 M hydroxylamine hydrochloride in 25% acetic acid	3 hours, repeat for 1.5 hours	90˚C	every 20 mins	Hall et al., 1996
E - Sulfides and Organics	**1st**: 3:2 30% hydrogen peroxide : 0.025 M HNO_3, **2nd**: 1.0 M ammonium acetate in 6% HNO_3	Heat until dry. Add **2nd** reagent for 30 mins	80˚C	**1st** reagent: none **2nd** reagent: constant	Papp et al., 1991
F - Residual	Total Digestion with HF-$HClO_4$-HNO_3-HCl	Performed at SGS (Toronto, Canada)			Hall et al., 1996

Step A of the sequential extraction was designed to remove cations electrostatically bonded to mineral surfaces by replacing these cations with others that will be more tightly bound to the mineral surface. According to Krauskopf and Bird (1995), cesium has a great ion affinity, meaning it should replace adsorbed cations. Also, some research suggests cesium chloride dissolves carbonates at a slower rate than other salt solutions used for the same purpose, such as ammonium chloride and magnesium chloride (Reardon et al., 1983). Therefore, 1.0 M CsCl was used to displace exchangeable cations as the first step in the sequential extraction procedure.

Carbonate Mineral Dissolution

Dissolution of carbonate phases was the next step (Step B) of this sequential extraction. Metals such as cadmium, copper, lead, uranium, zinc, and other divalent cations can either substitute for calcium in the crystal structure during precipitation or replace calcium after the crystals have formed (Hall, 1998). At the ZERT field site, a majority of the carbonates are secondary and occur in a plastic, fine grained, calcite-rich B horizon in the presence of a seasonally fluctuating water table, or as crusts on larger alluvial grains. When the water table rises above the B horizon in the wet winter months, metals in the groundwater can replace calcium in the crystal lattice. Also present in the ZERT sediment are detrital limestone and dolomite clasts, presumably from the Madison Formation that crops out in the Gallatin Mountains. Trace metals may have been incorporated into the crystal lattice of the calcite and dolomite during deposition of the Madison Limestone.

A majority of sequential extraction procedures are designed to dissolve carbonate phases using a sodium acetate-acetic acid buffer (Tessier et al., 1979; Chao, 1984; Maher, 1984; Hall, 1998). A 1.0 M sodium acetate solution adjusted to pH 5 with acetic acid is adequate for dissolution of the carbonate fraction in a soil with a weight percent of carbonate that is over half of the total sample (Hall, 1998). The carbonate-rich B horizon contains an estimated 15% calcite (unpublished data). Thus, this reagent should adequately dissolve the carbonates while still providing a margin for error. Caution must be used during this step because it has been shown that this reagent can attack minimal amounts of iron oxide minerals (Span and Gaillard, 1986).

Dissolution of Manganese Oxides and Amorphous Oxides

Metals associated with manganese oxides and amorphous iron and aluminum oxides were targeted in the third step (Step C) of the sequential procedure. These oxides commonly occur in oxygenated freshwater conditions as coatings on sediment grains or colloid-sized clusters. In addition, manganese oxides are poorly crystalline and are sometimes present in hydrous forms, thus making them more reactive (Chao and Theobald, 1976). Amorphous iron oxides are typically more prevalent than secondary manganese oxides; however, manganese oxides are strong "scavengers," which means they readily incorporate or possibly even concentrate metallic ions through adsorption, absorption, coprecipitation, and other processes, because Mn occurs in various valence states (Chao, 1984; Hall et al., 1996). Mn oxides often incorporate Fe, Zn, Pb, and Co (McKenzie, 1972; Chao and Theobald, 1976). This is especially the case for Co(III),

which easily replaces Mn(III) in the crystal lattice of partridgeite (Mn_2O_3) (McKenzie, 1972).

Secondary iron oxides and manganese oxides were of great importance to this study because of their mobility and reactivity, and it was of interest to extract them separately from crystalline iron oxides. For extraction step C, sediment residues from Step B were immersed in 0.25 M hydroxylamine hydrochloride - 0.25 M hydrochloric acid reagent for 2 h in a 60˚C water bath (Hall et al., 1996). A second leach with fresh reagent was carried out for another 30 min. Hall et al. (1996) showed that a second leach increases the total metallic concentration by 20%.

Crystalline Iron Oxide Dissolution

The next step (Step D) in this sequential extraction procedure pinpointed metals associated with crystalline iron oxides. Crystalline iron oxides are also important heavy metal accumulators, especially magnetite (Fe_2O_3), which is abundant in the ZERT sediment. Research has shown that magnetite commonly contains and sorbs heavy metals (Mayo et al., 2007). To extract cations from the crystalline oxides, the samples were subjected to 1.0 M hydroxylamine hydrochloride - 25% acetic acid at 90˚C for three h (Tessier et al., 1979; Hall et al., 1996). A second extraction with fresh reagent was carried out for 1.5 h. Hall et al. (1996) noticed an increase in metallic ion concentration of 15 – 20% with the second extraction.

Dissolution of Sulfide Minerals and Organic Matter

The next step (Step E) in the sequential extraction procedure targeted the organic humic substances and sulfide minerals in the soil. Sulfide minerals are a common trace component of igneous and metamorphic rocks, and sulfide minerals can contain a variety of metallic elements. However, sulfide minerals are also easily oxidized (Klein, 2002). Therefore, the concentration of sulfide minerals in detrital aquifer sediment may decrease with time.

Humic substances include humic acid, fulvic acid, and humin. These are long-lived, chemically resistant organic compounds that form during degradation of other organic matter (Schnitzer, 1978). Furthermore, humic substances are macromolecular and ubiquitous in soil and groundwater. Thus, they have the ability to contain high proportions of various metals. Metals can adsorb onto the organic matter, or they can chemically bind to the molecular structure, therefore making the organic matter an important source of trace metals (Schnitzer, 1978). Trace metals found to be huminophilic, which have the ability to sorb onto organic compounds, include sodium, potassium, calcium, strontium, barium, cesium, chromium, iron, cobalt, copper, zinc, uranium, and lead (Szalay, 1964). Many other metals are also chelated, or incorporated into the molecular structure of the organic compound. Chelated metals are tightly held and are most likely to be the main component of extraction Step E (Rashid, 1974).

Hydrogen peroxide is commonly used to remove metallic species associated with organic and sulfur compounds because it is a strong oxidizer (Tessier et al., 1979; Papp et al., 1991). Papp et al. (1991) evaluated a variety of methods for extracting metals from

oxides and sulfides; they found a 30% hydrogen peroxide – 0.025 M nitric acid reagent (3:2 volumetric ratio) to adequately extract metals from organic matter and sulfide minerals. An aliquot of this reagent was added to the residual sediment from the oxide extraction, which was then heated to 80˚C and left to evaporate until almost dry. At this point, 45 mL of 1.0 M ammonium acetate – 6% nitric acid solution were added to prevent sorption of compounds onto freshly oxidized surfaces (Tessier et al., 1979; Papp et al., 1991).

Residual Minerals

Finally, a near-total digestion of the residual sediment was executed to remove any remaining cations associated with silicate minerals (Step F). In addition, fresh sample aliquots were digested in a similar manner to determine the total elemental fractions in the sediment, designated as Step T in the data. Extraction residues and fresh sediment aliquots were digested by SGS (Toronto, Canada) using a four-acid digestion (HF-$HClO_4$-HNO_3-HCl), similar to that described by Hall et al. (1996). Their analysis required pulverization of the samples to 0.75 μm using a mill with an agate bowl to reduce metal contamination. The sum of the residual metals (Step F) and the metals extracted from each of the sequential steps (A through E) should equal the element totals (Step T) determined by the four-acid digestion. In addition, SGS also analyzed fresh sediment aliquots for organic and inorganic carbon contents.

Analysis of Supernate

All supernatants were analyzed using inductively coupled plasma mass spectrometry (ICP-MS). Inductively coupled plasma mass spectrometry is a method that involves heating a solution to such a degree that the compounds are reduced to ionized atoms. The masses and proportions of the ions are then determined using mass spectrometry. This detection technique is very sensitive and can be used for most elements. A major problem associated with the presented sequential extraction scheme is the tendency of acetate to form complex compounds with metal cations (Tessier et al., 1979). This is a problem that has yet to be solved, and the greatest implications are the loss of analytes detected and the creation of interferences in ICP-MS detection.

In addition to ICP-MS data, total digestion results from SGS Professional Laboratory (Ontario, Canada) were used. The sum of the element concentrations from each extraction step (A-E) and the near-total digestion (F) of the residual should equal the element concentrations from the near-total digestion of the virgin soil aliquot (T); the difference of these measures reflects the accuracy of the experiment. The precision was determined from sequentially extracting several aliquots of similar soil. Variation of the results is an indication of the heterogeneity of the soil and the repeatability of the experiment.

Experimental blanks consisted of reagent samples that were put through the extraction process without sediment. These reagents blanks reflect the cleanliness of the

reaction vessels and the purity of the reagents. All values are reported as milligrams or micrograms of metal per gram of soil (mg/g or ug/g).

RESULTS

Cation Concentrations and Recoveries

ICP-MS analysis yielded cation concentrations in each supernatant that were produced from the sequential extraction steps. These concentrations were important for determining the major, minor, and trace cations available in the sediment. The concentrations of selected cations are listed in tables 3 and 4. For data validation, a mass balance of the elements was determined by calculating metal recoveries.

Metal recoveries for each sample were determined by summing each metal from all of the extraction steps (A-F) and comparing it with the total (T) amount of metal determined in a fresh sediment sample, using the following equation:

$$\text{Recovery} = \frac{\sum_{i=A}^{F} [X]_i}{[X]_T} * 100\%$$

where [X] is the concentration of an element in mg/g of soil. This calculation was performed for each metal of each sample, and the results are given in tables 3 and 4 for W7 and W8, respectively. Here, and for the rest of the results and discussion, representative samples were chosen from the triplicate aliquots. ZRT-019 is shown for B horizon sediment, and ZRT-025 is shown for SSG sediment in Table 4. Concentrations that were too low to be detected are listed as being less than the lower limit of detection. Lower limits of detection were sensitive to the element analyzed, the calibration at the

Table 3. Element concentrations for each extraction step and recovery percentages of sequential extraction versus total extraction for selected cations from W7 sediment.

	W7 sediments	A	B	C	D	E	F	Sum A-F	T	% recovery
	Topsoil	3.52	0.89	1.47	0.12	0.22	11.4	17.6	15.8	*111*
Ca	B Horizon	2.51	36.63	6.64	0.16	0.23	15.4	61.6	68.6	*90*
(mg/g)	SSG	1.64	1.68	2.19	0.19	0.36	34.0	40.1	38.1	*105*
	DSG	1.49	1.55	2.10	0.18	0.39	33.9	39.6	37.8	*105*
	Topsoil	0.61	0.07	0.69	0.48	0.50	7.2	9.5	8.4	*114*
Mg	B Horizon	0.76	2.24	4.73	1.09	0.63	9.3	18.7	17.2	*109*
(mg/g)	SSG	0.27	0.05	1.23	0.50	0.23	14.3	16.6	16.1	*103*
	DSG	0.24	0.05	1.18	0.47	0.19	13.6	15.7	15.1	*104*
	Topsoil	< 0.01	< 0.01	2.48	2.26	0.42	28.8	34.0	30.1	*113*
Fe	B Horizon	< 0.01	< 0.01	1.81	2.46	0.16	29.7	34.1	29.7	*115*
(mg/g)	SSG	< 0.01	0.01	2.24	1.43	0.07	50.7	54.4	51.4	*106*
	DSG	< 0.01	0.03	2.37	1.47	0.07	48.4	52.3	50.4	*104*
	Topsoil	0.63	16.2	476	21.0	9.04	278	801	708	*113*
Mn	B Horizon	0.03	49.5	233	21.5	9.25	314	627	569	*110*
(ug/g)	SSG	< 0.01	10.8	150	17.6	4.50	775	958	926	*103*
	DSG	< 0.01	18.8	147	21.0	4.35	741	932	879	*106*
	Topsoil	< 0.1	0.16	5.02	2.14	0.26	18.3	25.9	22.1	*117*
Cu	B Horizon	< 0.1	0.89	5.48	3.59	0.30	14.3	24.6	20.2	*122*
(ug/g)	SSG	< 0.1	0.80	3.69	1.52	0.18	27.5	33.7	21.2	*159*
	DSG	< 0.1	1.17	4.11	1.55	0.19	17.2	24.2	20.7	*117*
	Topsoil	0.06	0.07	0.21	< 0.02	< 0.01	0.05	0.39	0.33	*118*
Cd	B Horizon	< 0.03	0.15	0.03	< 0.02	< 0.01	0.04	0.22	0.26	*84*
(ug/g)	SSG	< 0.03	< 0.02	0.03	< 0.02	< 0.01	0.06	0.09	0.11	*82*
	DSG	< 0.03	< 0.02	0.03	< 0.02	< 0.01	0.06	0.09	0.10	*89*
	Topsoil	< 0.1	< 0.1	9.67	3.94	2.37	81	97	77	*126*
Zn	B Horizon	< 0.1	0.15	7.56	5.93	2.53	56	72	61	*118*
(ug/g)	SSG	< 0.1	< 0.1	5.73	0.17	1.18	88	95	83	*115*
	DSG	< 0.1	< 0.1	5.49	< 0.1	0.91	79	85	83	*103*
	Topsoil	< 0.02	0.24	11.1	1.61	0.11	13.0	26.1	20.5	*127*
Pb	B Horizon	< 0.02	0.86	6.24	1.46	0.10	11.9	20.6	18.8	*109*
(ug/g)	SSG	< 0.02	0.30	2.25	0.51	0.07	16.6	19.7	17.8	*111*
	DSG	< 0.02	1.20	4.01	0.51	0.09	16.6	22.4	30.6	*73*
	Topsoil	< 0.1	< 1.0	0.94	< 0.8	0.21	7	8	8	*102*
As	B Horizon	< 0.1	< 1.0	0.59	< 0.8	< 0.2	6	7	7	*94*
(ug/g)	SSG	< 0.1	< 1.0	< 0.4	< 0.8	< 0.2	1	1	2	*50*
	DSG	< 0.1	< 1.0	< 0.4	< 0.8	< 0.2	2	2	1	*200*
	Topsoil	< 0.02	0.05	0.17	0.06	0.15	2.05	2.48	2.24	*111*
U	B Horizon	< 0.02	0.13	0.17	0.06	0.07	1.95	2.39	2.05	*117*
(ug/g)	SSG	< 0.02	0.03	0.13	0.02	0.02	1.51	1.71	1.57	*109*
	DSG	< 0.02	0.03	0.13	0.01	0.02	1.44	1.63	1.62	*100*
	Topsoil	< 0.3	< 0.4	2.47	3.44	4.93	51	62	63	*98*
Cr	B Horizon	< 0.3	< 0.4	1.18	0.57	2.02	56	60	61	*98*
(ug/g)	SSG	< 0.3	< 0.4	1.31	0.96	0.49	80	83	82	*101*
	DSG	< 0.3	1.14	2.31	1.49	0.69	68	74	69	*107*
	Topsoil	34.3	27.9	71.3	21.6	5.45	702	863	778	*111*
Ba	B Horizon	28.1	72.0	31.5	17.7	4.59	730	884	762	*116*
(ug/g)	SSG	16.7	12.4	24.2	7.34	5.24	1520	1586	1510	*105*
	DSG	18.9	12.6	30.3	8.95	6.26	1540	1617	1560	*104*

Table 4. Element concentrations for each extraction step and recovery percentages of sequential extraction versus total extraction for selected cations from W8 sediment.

	W8 samples	A	B	C	D	E	F	Sum A-F	T	% recovery
	Topsoil	3.94	1.10	1.62	0.11	0.27	10.9	17.9	16.5	*109*
Ca	B Horizon	2.56	15.47	5.51	0.25	0.52	21.7	46.0	50.1	*92*
(mg/g)	SSG	1.39	1.66	2.09	0.20	0.47	32.6	38.4	41.2	*93*
	DSG	1.54	0.26	1.91	0.21	0.46	31.5	35.9	32.9	*109*
	Topsoil	0.73	0.09	0.79	0.50	0.77	8.2	11.1	8.7	*127*
Mg	B Horizon	0.65	0.58	4.03	0.87	0.62	11.4	18.2	18.2	*100*
(mg/g)	SSG	0.25	0.07	1.37	0.44	0.30	13.5	15.9	16.9	*94*
	DSG	0.28	0.04	1.23	0.44	0.27	13.2	15.5	14.1	*110*
	Topsoil	< 0.06	< 0.1	2.51	2.21	0.91	30.4	36.0	30.5	*118*
Fe	B Horizon	< 0.06	< 0.1	2.14	2.10	0.26	38.2	42.7	45.3	*94*
(mg/g)	SSG	< 0.06	< 0.1	2.34	1.22	0.11	47.3	51.0	55.0	*93*
	DSG	< 0.06	< 0.1	2.68	1.35	0.10	45.4	49.5	45.0	*110*
	Topsoil	0.57	17.1	443	17.0	14.4	272	764	679	*113*
Mn	B Horizon	0.07	30.3	248	21.0	9.94	519	828	830	*100*
(ug/g)	SSG	0.24	12.8	162	17.1	7.91	744	944	985	*96*
	DSG	< 0.01	16.9	271	20.0	6.89	731	1046	876	*119*
	Topsoil	< 0.1	0.14	5.66	2.17	0.34	20.1	28.4	22.5	*126*
Cu	B Horizon	< 0.1	0.76	6.71	2.49	0.46	13.6	24.0	27.0	*89*
(ug/g)	SSG	< 0.1	4.00	5.81	1.31	0.32	16.4	27.8	29.3	*95*
	DSG	< 0.1	1.11	5.26	1.48	0.23	16.5	24.6	23.7	*104*
	Topsoil	0.04	0.10	0.35	< 0.02	< 0.01	0.08	0.57	0.43	*131*
Cd	B Horizon	< 0.03	0.23	0.07	< 0.02	< 0.01	0.05	0.35	0.18	*194*
(ug/g)	SSG	0.6	0.45	0.09	< 0.02	< 0.01	0.05	1.14	0.10	*1136*
	DSG	0.46	0.48	0.14	< 0.02	< 0.01	0.08	1.16	0.11	*1055*
	Topsoil	< 0.1	< 0.1	12.2	5.01	7.91	69	94	81	*116*
Zn	B Horizon	< 0.1	< 0.1	7.65	2.94	3.36	67	81	79	*102*
(ug/g)	SSG	< 0.1	0.9	6.84	< 0.1	2.26	73	83	87	*95*
	DSG	< 0.1	< 0.1	6.73	< 0.1	1.84	68	77	78	*98*
	Topsoil	< 0.02	0.43	14.2	1.35	0.09	12.1	28.2	24.3	*116*
Pb	B Horizon	< 0.02	0.38	5.96	1.31	0.21	12.8	20.7	17.0	*122*
(ug/g)	SSG	< 0.02	3.01	6.75	0.55	0.06	20.1	30.5	24.0	*127*
	DSG	< 0.02	1.81	9.24	0.54	0.05	16.0	27.6	25.3	*109*
	Topsoil	< 1.0	< 0.6	0.78	< 0.8	< 0.2	7	8	8	*97*
As	B Horizon	< 1.0	< 0.6	< 0.4	< 0.8	< 0.2	3	3	4	*75*
(ug/g)	SSG	< 1.0	< 0.6	< 0.4	< 0.8	< 0.2	1	1	2	*50*
	DSG	< 1.0	< 0.6	< 0.4	< 0.8	< 0.2	2	2	1	*200*
	Topsoil	< 0.02	0.04	0.20	0.08	0.16	2.04	2.53	2.15	*117*
U	B Horizon	< 0.02	0.07	0.18	0.04	0.06	1.67	2.03	1.87	*108*
(ug/g)	SSG	< 0.02	0.02	0.13	0.02	0.03	1.50	1.68	1.63	*103*
	DSG	< 0.02	0.02	0.13	0.01	0.02	1.37	1.55	1.52	*102*
	Topsoil	< 0.3	< 0.4	2.95	4.42	6.32	58	72	66	*109*
Cr	B Horizon	< 0.3	0.43	1.16	4.64	1.64	82	90	83	*108*
(ug/g)	SSG	< 0.3	1.01	2.06	1.84	0.62	65	71	80	*88*
	DSG	< 0.3	1.17	3.82	3.39	0.90	56	65	64	*102*
	Topsoil	57.9	20.2	63.2	17.9	7.62	699	866	734	*118*
Ba	B Horizon	35.6	30.3	41.8	16.1	8.28	1025	1157	1110	*104*
(ug/g)	SSG	18.4	6.9	32.8	7.07	7.11	1530	1602	1590	*101*
	DSG	23.9	9.8	36.5	6.74	6.47	1410	1493	1440	*104*

time of analysis, and the dilution factor of the analyte. The dilution factor was directly related to the type of reagent used; organic reagents such as ammonium acetate used in Step E required little dilution for ICP-MS analysis, whereas the cesium chloride and sodium acetate solutions had dominant alkaline cations, which created the danger of overwhelming the ICP-MS detector unless diluted sufficiently.

On average, the recoveries of the sequential extractions were about 10% higher than the total extractions. Differences from 100% recovery were attributed to cations whose concentrations were close to lower detection limits, as was the case for arsenic, those that were predominantly found in Step F, like copper, or the fact that fresh sediment aliquots sent to SGS were inherently different than those that underwent the sequential extraction procedure. For elements with concentrations very close to detection limits such as cadmium, the heterogeneity may account for the greater than 10% discrepancy from 100% recovery. There may also be other cadmium contamination that was not distinguishable with the sequential extraction. Another factor that might have contributed to imperfect recoveries was that SGS pulverized the samples and used a much smaller mass for analysis. Finally, SGS warned that a four-acid digestion has the potential for metal loss through volatilization or precipitation. There may be metal losses for arsenic, aluminum, barium, chromium, manganese, and lead. However, a 10% difference in recoveries reflected acceptable accuracy.

Both strontium and cobalt concentrations were also determined during analysis, but they are not shown in tables 3 or 4 because they are less harmful to human health. However, Sr and Co were important for the discussion of the results, and their

concentrations are shown in later tables. The lower limit of detection for both Sr and Co was typically very low, less than 0.02 ug/g.

Several elements (Li, Na, Al, Si, K, and Mo) were also included in the analysis of the sequential extraction and total extraction samples; however, these elements were omitted from the results and discussion. Lithium, cobalt, and molybdenum were omitted because these elements were of minimal concern to human health, and these elements were below detection limits in most samples. Lithium and molybdenum had detection limits in the range of 0.05 to 0.2 ug/g, and the detection limit for cobalt was in the range of 0.01 to 0.02 ug/g. Sodium was not discussed in Steps B through D because the B Step reagent had high concentrations of sodium, which had a great influence on sodium concentrations in the analytes. Sodium had typical detection limits around or below 1.2 ug/g. Aluminum and silicon were ubiquitous in the mineral phases, and are thus not discussed in results. The lower limit of detection for aluminum fell within the range of 0.01 to 0.4 ug/g. Silicon and potassium had much higher detection limits in the range of 10 to 400 ug/g. Detection limits varied depending on the calibration of the ICP-MS, which varied daily. In addition, detection limits varied from element to element, and with each reagent.

Repeatability

The precision of the experiment was determined by comparing the results obtained from triplicate analyses. Three aliquots were analyzed from both the B horizon

and the SSG in W8. The precision was estimated by determining the mean and relative standard deviation (RSD) of the metal concentrations from the sequential extraction steps. A summary of the means and RSDs for these samples is found in tables 5 and 6.

Table 5. Mean concentrations and relative standard deviations (%) for metals in triplicate B horizon samples from W8. RSD values above 15% are bold, and blank values are below the lower limit of detection.

	Ca (mg/g)	Mg (mg/g)	Fe (mg/g)	Mn (mg/g)	Cr (ug/g)
Step A	2.57 ± 2.4%	0.66 ± 1.1%	-	-	-
Step B	16.1 ± 3.5%	0.61 ± 4.8%	-	0.03 ± 6.3%	0.35 ± **71.6**%
Step C	5.48 ± 1.4%	4.07 ± 3.6%	2.20 ± 6.9%	0.23 ± 12.5%	1.19 ± 4.7%
Step D	0.24 ± 3.4%	0.84 ± 5.9%	2.06 ± 2.0%	0.02 ± 4.0%	4.52 ± 10.1%
Step E	0.49 ± 6.9%	0.60 ± 5.3%	0.23 ± **21.3**%	0.01 ± 2.0%	1.73 ± 4.6%

	Co (ug/g)	Zn (ug/g)	Cu (ug/g)	Sr (ug/g)	Ba (ug/g)
Step A	-	-	-	15.4 ± 6.2%	34.7 ± 3.1%
Step B	0.04 ± 6.1%	-	0.75 ± 13.1%	24.3 ± 1.5%	29.7 ± 2.9%
Step C	3.59 ± 1.7%	7.91 ± 7.1%	6.59 ± 2.5%	8.13 ± 2.3%	41.8 ± 0.7%
Step D	0.86 ± 3.0%	3.13 ± 7.0%	2.50 ± 3.9%	3.32 ± 1.1%	16.1 ± 3.3%
Step E	0.45 ± 10.7%	2.97 ± **20.1**%	0.39 ± **24.2**%	6.45 ± **15.9**%	7.73 ± 6.5%

	Pb (ug/g)	U (ug/g)	Cd (ug/g)
Step A	-	-	-
Step B	0.37 ± 2.3%	0.07 ± 5.5%	0.38 ± **82.7**%
Step C	5.71 ± 4.8%	0.17 ± 8.3%	0.10 ± **58.0**%
Step D	1.29 ± 10.3%	0.04 ± **18.8**%	-
Step E	0.16 ± **40.2**%	0.06 ± 1.8%	-

A RSD of less than 15% was considered acceptable. Metals with greater RSDs reflected the fact that the sediment was very heterogeneous and some metal-bearing minerals occurred so sparsely that they were not found in each sample, especially for shallow and deep sandy-gravel sediment. This was difficult to distinguish from

Table 6. Mean concentrations and relative standard deviations (%) for metals in triplicate shallow sandy gravel (SSG) samples from W8. RSD values above 15% are bold, and blank spaces reflect values below the lower limit of detection.

	Ca (mg/g)	Mg (mg/g)	Fe (mg/g)	Mn (mg/g)	Cr (ug/g)
Step A	1.37 ± 4.1%	0.24 ± 7.7%	-	-	-
Step B	1.87 ± **33.7**%	0.07 ± 5.4%	-	0.01 ± 13.2%	1.11 ± **31.3**%
Step C	2.25 ± 6.8%	1.35 ± 1.2%	2.29 ± 2.0%	0.16 ± 9.6%	2.29 ± 13.9%
Step D	0.23 ± **21.4**%	0.47 ± 6.0%	1.29 ± 5.7%	0.02 ± 3.7%	3.30 ± **47.3**%
Step E	0.55 ± **21.0**%	0.33 ± 7.8%	0.11 ± **28.1**%	0.01 ± **31.7**%	0.81 ± **21.9**%

	Co (ug/g)	Zn (ug/g)	Cu (ug/g)	Sr (ug/g)	Ba (ug/g)
Step A	-	-	-	7.03 ± 8.4%	19.4 ± 4.9%
Step B	0.02 ± 14.8%	0.87 ± 5.9%	4.29 ± 5.9%	1.72 ± 10.5%	7.71 ± 9.6%
Step C	2.36 ± 1.0%	6.97 ± 2.5%	5.92 ± 1.8%	6.76 ± **17.0**%	31.0 ± 8.0%
Step D	0.64 ± 12.7%	-	1.38 ± 4.3%	1.97 ± **20.1**%	7.90 ± 9.5%
Step E	0.35 ± 8.0%	1.99 ± **19.8**%	0.33 ± **27.6**%	6.40 ± 10.9%	7.04 ± 1.5%

	Pb (ug/g)	U (ug/g)	Cd (ug/g)
Step A	-	-	0.34 ± **79.7**%
Step B	3.12 ± 3.8%	0.02 ± **26.6**%	0.33 ± **67.1**%
Step C	6.75 ± 1.5%	0.13 ± 5.1%	0.07 ± **41.3**%
Step D	0.59 ± 9.9%	0.02 ± **29.9**%	-
Step E	0.06 ± **22.2**%	0.03 ± 7.7%	-

contamination of the sample, which also increases the RSD. Heterogeneity or contamination may explain the high RSD values for chromium in Step B, and possibly some of the cadmium concentrations. Furthermore, some metals are close to the detection limit, which increases the RSD. This was the case for cadmium in most samples, uranium in the Step D sample, and many of the metals analyzed in Step E samples. In general, a majority of the RSD values reflected acceptable precision and repeatability of the experiment.

Metal Speciation

Cations Associated with Ion Exchange

Table 7 lists the exchangeable cations in the ZERT sediment that were extracted in Step A. The exchange fraction was dominated by major cations including calcium, magnesium, and sodium, but lower concentrations of manganese, strontium, barium, and cadmium were obtained. ICP-MS is only suitable for low total dissolved solid concentrations (~300 mg/L), and the initial cesium chloride solution was ~170,000 mg/L. Thus, the extraction solutions had to be diluted to a large degree for analysis. Therefore, this excluded the detection of cations with high limits of detection, such as potassium,

Table 7. Exchangeable cations determined in Step A of the sequential extraction. Non-detected values are those that are below the lower limit of detection, and are indicated as less than the detection limit.

Sample	Z-003	Z-015	Z-006	Z-018	Z-019	Z-020	Z-102	Z-024	Z-025	Z-026	Z-104	Z-029
Well	W7	W8	W7	W8	W8	W8	W7	W8	W8	W8	W7	W8
Soil Type	Topsoil	Topsoil	B Hor.	B Hor.	B Hor.	B Hor.	SSG	SSG	SSG	SSG	DSG	DSG
Major Cations (mg/g)												
Ca	3.52	3.94	2.51	2.51	2.56	2.64	1.64	1.31	1.39	1.42	1.49	1.54
Mg	0.61	0.73	0.76	0.66	0.65	0.67	0.27	0.22	0.25	0.26	0.24	0.28
Na	0.02	0.02	0.03	0.03	0.04	0.03	0.02	0.02	0.02	0.02	0.02	0.03
Minor and Trace Cations (µg/g)												
Mn	0.63	0.57	0.03	0.17	0.07	0.12	< 0.01	0.23	0.24	0.19	< 0.01	< 0.01
Sr	13.0	21.3	12.2	15.8	16.0	14.3	4.77	7.58	6.41	7.12	4.30	6.87
Ba	34.3	57.9	28.1	34.8	35.6	33.5	16.7	19.8	18.4	20.1	18.9	23.9
Cd	0.06	0.04	< 0.03	< 0.03	< 0.03	0.17	< 0.03	< 0.03	0.55	0.45	< 0.03	0.46
CEC (meq/100g)												
	22.7	25.8	19.0	18.2	18.4	18.9	10.5	8.5	9.1	9.4	9.5	10.2

and other elements that were a small fraction of the sorbed elements and thus occurred in low concentrations, including most of the trace and toxic metals.

The cation concentrations were used to determine the cation exchange capacity (CEC) of the sediment samples (Table 7). CEC is a commonly used comparison tool in soil chemistry. Malcolm and Kennedy (1970) reported CEC values near 8 meq/100 g for sieved sand, 11 meq/100 g for sieved silt, and 36 meq/100 g for sieved clay, all with organic carbon intact. Considering that the ZERT soil samples were not sieved below a grain size of 2 mm, the CEC values seemed to be reasonable. Fine-grained, organic-rich samples, such as topsoil and B horizon samples, had high CEC values (18.2 – 25.8 meq/100g), and coarser, sandy gravel samples (SSG and DSG) showed a markedly lower CEC (8.5 to 10.5 meq/100g). Due to a mix up of analytes during Step A, W7 SSG and W7 DSG samples had to be repeated. Therefore, for Step A only, sample ZRT-009 was replaced by ZRT-102, and ZRT-012 was replaced by ZRT-104.

Cations Associated with Carbonate Dissolution

Carbonate species were targeted in Step B of the sequential extraction, and Table 8 summarizes the cation concentrations found in each sample. The major cations associated with carbonate minerals in the ZERT samples were calcium and magnesium, along with minor elements such as strontium and barium. Due to the high concentration of sodium in the reagent and limitations of ICP-MS, sodium concentrations were not analyzed. Also, as with Step A extracts, these samples required high dilution ratios, thus making some trace elements difficult to detect. However, more elements were detected

in Step B than Step A. The detection limits of elements in Step B were similar to those found in Step A, thus the increase in detected elements was from the release of these elements during dissolution of carbonate minerals.

The inorganic carbon content determined using coulometry by SGS was 1.3 – 2.0 mg/g in topsoil, 27 – 68 mg/g for B horizon sediment, and 0.8 – 3.7 mg/g for sandy gravel samples. Table 9 shows the inorganic carbon in fresh sediment determined in fresh sediment aliquots by SGS in addition to calcium and magnesium concentrations determined in Step B of the sequential extraction. The first column in table 9 lists the concentration of inorganic carbon in a fresh sediment aliquot determined by SGS. Also

Table 8. Cations associated with the dissolution of carbonate phases in Step B of the sequential extraction.

Sample	Z-003	Z-015	Z-006	Z-018	Z-019	Z-020	Z-009	Z-024	Z-025	Z-026	Z-012	Z-029
Well	W7	W8	W7	W8	W8	W8	W7	W8	W8	W8	W7	W8
Soil Type	Topsoil	Topsoil	B Hor.	B Hor.	B Hor.	B Hor.	SSG	SSG	SSG	SSG	DSG	DSG
Major Cations (mg/g)												
Ca	0.89	1.10	36.6	16.6	15.5	16.1	1.68	2.57	1.66	1.36	1.55	0.26
Mg	0.07	0.09	2.24	0.63	0.58	0.62	0.05	0.07	0.07	0.07	0.05	0.04
Fe	< 0.01	< 0.01	< 0.01	< 0.01	< 0.01	< 0.01	0.01	< 0.01	0.03	0.03	0.03	0.03
Minor and Trace Cations (µg/g)												
Mn	16.2	17.1	49.5	33.4	30.3	34.2	10.8	12.0	12.8	15.4	18.8	16.9
Al	7.33	4.59	45.0	40.1	27.5	42.9	34.5	30.7	39.7	40.2	46.7	54.8
Cr	< 0.4	< 0.4	< 0.4	< 0.4	0.43	0.54	< 0.4	0.82	1.01	1.49	1.14	1.17
Co	0.02	0.02	0.12	0.04	0.04	0.04	0.01	0.02	0.02	0.02	0.06	0.01
Cu	0.16	0.14	0.89	0.65	0.76	0.85	0.80	4.46	4.00	4.42	1.17	1.11
Sr	5.71	4.04	59.2	24.2	23.9	24.6	2.55	1.79	1.85	1.51	1.99	0.63
Ba	27.9	20.2	72.0	30.1	30.3	28.7	12.4	8.32	6.89	7.90	12.6	9.79
Cd	0.07	0.10	0.15	0.17	0.23	0.74	< 0.02	0.07	0.45	0.46	< 0.02	0.48
Pb	0.24	0.43	0.86	0.36	0.38	0.38	0.30	3.25	3.01	3.09	1.20	1.81
U	0.05	0.04	0.13	0.07	0.07	0.08	0.03	0.02	0.02	0.01	0.03	0.02

Table 9. Inorganic carbon content determined by SGS compared with the calcium and magnesium concentrations determined in sequential extraction Step B. Assuming these ions are the result of calcite and magnesite dissolution, then there is more inorganic carbon in the sediment than would be produced during dissolution. The excess amount of inorganic carbon is listed in the last columns.

	Inorganic Carbon CO_2		Calcium Ca	Calcium CaO	Magnesium Mg	Magnesium MgO	Inorganic Carbon Leftover CO_2	
	(mg/g)†	(mol/g)	(mg/g)	(mol/g)	(mg/g)	(mol/g)	(mg/g)	(mol/g)
W7								
Topsoil	1.3	2.96E-05	0.89	2.21E-05	0.07	2.80E-06	0.20	4.61E-06
B Horizon	68.2	1.55E-03	36.6	9.14E-04	2.24	9.21E-05	23.9	5.44E-04
SSG	3.0	6.82E-05	1.68	4.20E-05	0.05	2.14E-06	1.06	2.40E-05
DSG	2.6	5.91E-05	1.55	3.87E-05	0.05	2.19E-06	0.80	1.82E-05
W8								
Topsoil	2.0	4.55E-05	1.10	2.76E-05	0.09	3.83E-06	0.62	1.41E-05
B Horizon	27.2	6.18E-04	15.5	3.86E-04	0.58	2.37E-05	9.18	2.09E-04
SSG	3.7	8.41E-05	1.66	4.15E-05	0.07	3.04E-06	1.74	3.96E-05
DSG	0.8	1.82E-05	0.26	6.51E-06	0.04	1.50E-06	0.45	1.02E-05

†Values from SGS

listed are concentrations of calcium and magnesium determined in Step B of the sequential extraction. The amount of carbonate that could have produced these concentrations of calcium and magnesium was also calculated by treating the calcium as having been produced by calcite dissolution, and the magnesium having been produced from magnesite dissolution. However, it is more likely that magnesium-calcite or dolomite was in the soil. Finally, the amount of inorganic carbon that would remain is listed in the final column. In all samples, there was more inorganic carbon than cations than could be accounted for with dissolution of carbonate minerals. While there could be some differences due to heterogeneities of the soil aliquots, it is also likely that not all of

the carbonate minerals were dissolved during Step B, which will be discussed further in Step C results.

Table 10 shows the correlations of selected elements with calcium and iron. These data suggested that magnesium, strontium, barium, cobalt, and uranium were associated with carbonate minerals. The slope was calculated by taking a linear regression through the molar concentration of a major element and the molar concentration of a minor or trace element that was linearly related, for all samples within each extraction step. The correlation factor, r, is the Pearson coefficient, which indicated positive correlations and was useful for determining the critical correlation factor. Statistically, the critical correlation factor provides a confidence interval. Above the critical correlation value, it was reasonable to assume that the linearity of the data was not a random occurrence.

Table 10. Cation correlations from Step B of the sequential extraction.

Calcium Correlations	r	Slope (mol/mol)	Iron Correlations	r	Slope (mol/mol)
Mg	0.97	9.11×10^{-2}	*Al*	*0.65* †	*1.17×10^{0}*
Sr	0.99	7.19×10^{-4}	Cd	1.00††	1.16×10^{-2}
Ba	0.92	4.41×10^{-4}			
Mn	0.97	7.52×10^{-4}			
Co	0.84	1.60×10^{-6}			
U	0.95	5.12×10^{-7}			

Critical correlation value for a 10% confidence level with 12 samples is 0.497.

†Critical correlation value for a 10% confidence level with 5 samples is 0.805.

††Critical correlation value for a 10% confidence level with 3 samples is 0.988.

There were also a few iron correlations in Step B. Iron, aluminum, and cadmium were closely related without being correlated with calcium. Even though the correlation between iron and aluminum was not above the critical correlation value, aluminum was listed in Table 10 because it showed an almost one to one molar ratio with iron. This implied that a small amount of iron and aluminum oxides were dissolving in Step B with slightly depressed pH values, which was similar to the results reported by Span and Gaillard (1986). However, only a small amount of the total iron was extracted in Step B, at most 0.06%; thus, this step remained devoted to carbonate mineral dissolution. It is also worth noting that the iron was strongly correlated with cadmium.

Cations Associated with Manganese Oxides and Amorphous Oxides

Cations associated with manganese oxides and amorphous iron and other oxides are found in Table 11. The minerals targeted include but are not limited to pyrolusite, hausmannite, brucite, goethite, lepidochrosite, and limonite. The most common cation correlations occurred with manganese and iron. Iron oxides are typically more prevalent than manganese oxides, so it was not surprising that there was more iron than manganese. However, because the iron concentrations were high (1.8 -2.7 mg/g), it is possible that some of the crystalline iron oxides targeted in Step D were actually affected in Step C. Regardless, many of the trace metals correlated more closely with manganese than iron, so it was inferred that these metals were released primarily as a result of manganese oxide dissolution. This was reasonable because manganese oxides are heavy metal scavengers as described in the methods section.

Table 11. Cation concentrations from manganese oxides and amorphous oxides determined in Step C of the sequential extraction.

Sample	Z-003	Z-015	Z-006	Z-018	Z-019	Z-020	Z-009	Z-024	Z-025	Z-026	Z-012	Z-029
Well	W7	W8	W7	W8	W8	W8	W7	W8	W8	W8	W7	W8
Soil Type	Topsoil	Topsoil	B Hor.	B Hor.	B Hor.	B Hor.	SSG	SSG	SSG	SSG	DSG	DSG
Major Cations (mg/g)												
Ca	1.47	1.62	6.64	5.39	5.51	5.54	2.19	2.26	2.09	2.39	2.10	1.91
Mg	0.69	0.79	4.73	3.95	4.03	4.23	1.23	1.34	1.37	1.34	1.18	1.23
K	0.21	0.29	0.08	0.10	0.11	0.12	0.07	0.08	0.09	0.08	0.07	0.09
Al	2.29	2.56	1.61	1.84	1.89	1.91	1.21	1.15	1.13	1.16	1.20	1.48
Fe	2.48	2.51	1.81	2.10	2.14	2.38	2.24	2.25	2.34	2.28	2.37	2.68
Mn	0.48	0.44	0.23	0.25	0.25	0.20	0.15	0.15	0.16	0.18	0.15	0.27
Minor and Trace Cations (µg/g)												
Li	1.42	1.36	2.76	1.60	1.63	1.78	0.68	0.84	0.77	0.91	0.67	0.72
Cr	2.47	2.95	1.18	1.16	1.16	1.25	1.31	2.16	2.06	2.66	2.31	3.82
Co	5.30	5.06	3.32	3.52	3.61	3.64	2.52	2.36	2.35	2.39	2.28	3.07
Zn	9.67	12.2	7.56	7.53	7.65	8.55	5.73	7.17	6.84	6.89	5.49	6.73
Cu	5.02	5.66	5.48	6.41	6.71	6.66	3.69	5.92	5.81	6.02	4.11	5.26
As	0.94	0.78	0.59	0.48	< 0.4	0.44	< 0.4	< 0.4	< 0.4	< 0.4	< 0.4	< 0.4
Sr	6.78	6.25	8.07	8.08	7.97	8.34	6.07	6.12	6.06	8.09	5.56	6.56
Ba	71.3	63.2	31.5	42.0	41.8	41.4	24.2	28.2	32.8	32.0	30.3	36.5
Cd	0.21	0.35	0.03	0.06	0.07	0.16	0.03	0.04	0.09	0.09	0.03	0.14
Pb	11.1	14.2	6.24	5.41	5.96	5.74	2.25	6.66	6.75	6.86	4.01	9.24
U	0.17	0.20	0.17	0.16	0.18	0.15	0.13	0.12	0.13	0.14	0.13	0.13

Table 12 shows correlations between trace metals and manganese, iron, or calcium. Many trace metals including barium, cobalt, and lead, among others, showed linear relationships with manganese. From this it can be inferred that these trace metals were released primarily as a result of manganese oxide dissolution. Iron concentrations were closely correlated with chromium concentrations. Stainless steel contains approximately 10% chromium by mass, which is greater than the ratio of iron to chromium shown in Table 12. Therefore, this is inferred to be a truly linear relationship from amorphous iron oxide dissolution rather than contamination. Finally, calcium was

Table 12. Cation correlations for Step C, manganese oxides and amorphous oxides.

Manganese Correlations	r	Slope (mol/mol)	Iron Correlation	r	Slope (mol/mol)
Al	0.88	7.85×10^{0}	Cr	0.80	3.31×10^{-3}
Ba	0.95	4.87×10^{-2}			
Zn	0.84	1.15×10^{-2}	Calcium Correlations	r	Slope (mol/mol)
Pb	0.85	6.48×10^{-3}	Mg	1.0	1.34×10^{0}
Co	0.95	8.22×10^{-3}	Li	0.82	1.56×10^{-3}
As	0.93†	1.22×10^{-3}	Sr	0.80	1.98×10^{-4}
Cd	0.82	3.47×10^{-4}			
U	0.75	4.10×10^{-5}			

Critical correlation value for a 10% confidence level with 12 samples is 0.497.
†Critical correlation value for a 10% confidence level with 5 samples is 0.805.

correlated with magnesium, lithium, and strontium in the sediment and it is possible this was the result of dolomite dissolution.

Table 13 shows the leftover inorganic carbon content in the sediment determined from Step B as well as the magnesium and calcium concentrations determined in Step C supernatants of the sequential extraction. These concentrations were converted to molar ratios of inorganic carbon (CO_2), calcium oxide (CaO), and magnesium oxide (MgO). In dolomite ($CaMg(CO_3)_2$), these three components would occur in equal molar ratios (CO_2:CaO:MgO would be 1:1:1). Using this ratio, the amount of dolomite that could have dissolved was determined from the limiting component that had the lowest concentration. In all sediment samples, except the B horizon, the concentrations of calcium and magnesium in this extraction step adequately accounted for the excess inorganic carbon not accounted for in Step B. From this it was implied that carbonate

dissolution continued during Step C. Calcium and magnesium occurred in similar molar concentrations (Ca vs Mg slope = 1.34, Table 12), signaling the dissolution of dolomite. However, dolomite dissolution does not account for all of the calcium and magnesium cations. This could be the result of heterogeneities in the inorganic carbon content of the sediment samples, or calcium and magnesium minerals in addition to dolomite were dissolving during Step C.

Table 13. Calculation of the amount of dolomite that could have dissolved in Step C. Also included are the concentrations of calcium and magnesium cations extracted during Step C, and the excess inorganic carbon from Step B (Table 9).

	Inorganic Carbon Leftover[†] CO_2		Calcium Ca	Calcium CaO	Magnesium Mg	Magnesium MgO	Amount of Dolomite that Could have Dissolved $CaMg(CO_3)_2$
	(mg/g)	(mol/g)	(mg/g)	(mol/g)	(mg/g)	(mol/g)	(mol/g)
W7							
Topsoil	0.20	4.61E-06	1.47	3.67E-05	0.69	2.84E-05	4.61E-06
B Horizon	23.9	5.44E-04	6.64	1.66E-04	4.73	1.94E-04	1.66E-04
SSG	1.06	2.40E-05	2.19	5.47E-05	1.23	5.04E-05	2.40E-05
DSG	0.80	1.82E-05	2.10	5.25E-05	1.18	4.83E-05	1.82E-05
W8							
Topsoil	0.62	1.41E-05	1.62	4.03E-05	0.79	3.25E-05	1.41E-05
B Horizon	9.18	2.09E-04	5.51	1.37E-04	4.03	1.66E-04	1.37E-04
SSG	1.74	3.96E-05	2.09	5.21E-05	1.37	5.64E-05	3.96E-05
DSG	0.45	1.02E-05	1.91	4.77E-05	1.23	5.07E-05	1.02E-05

[†]From Table 9

Cations Associated with Crystalline Iron Oxides

Crystalline oxide minerals, mostly iron oxides such as magnetite and hematite, were dissolved in Step D. The cations associated with these minerals are listed in Table 14. There was a great deal of iron (1.2 – 2.5 mg/g) leached in this extraction step. This

Table 14. Cations associated with iron oxide minerals determined in Step D of the sequential extraction.

Sample	Z-003	Z-015	Z-006	Z-018	Z-019	Z-020	Z-009	Z-024	Z-025	Z-026	Z-012	Z-029
Well	W7	W8	W7	W8	W8	W8	W7	W8	W8	W8	W7	W8
Soil Type	Topsoil	Topsoil	B Hor.	B Hor.	B Hor.	B Hor.	SSG	SSG	SSG	SSG	DSG	DSG
Major Cations (mg/g)												
Ca	0.12	0.11	0.16	0.24	0.23	0.24	0.19	0.21	0.20	0.29	0.18	0.21
Mg	0.48	0.50	1.09	0.85	0.87	0.78	0.50	0.49	0.44	0.47	0.47	0.44
K	0.23	0.26	0.11	0.10	0.09	0.10	0.04	0.04	0.04	0.03	0.04	0.02
Al	0.84	0.83	0.87	0.59	0.60	0.62	0.29	0.45	0.27	0.28	0.28	0.37
Fe	2.26	2.21	2.46	2.07	2.10	2.02	1.43	1.36	1.22	1.28	1.47	1.35
Mn	0.02	0.02	0.02	0.02	0.02	0.02	0.02	0.02	0.02	0.02	0.02	0.02
Minor and Trace Cations (µg/g)												
Li	1.53	1.83	1.89	1.14	1.20	1.11	0.67	0.40	0.40	0.24	0.28	0.47
Cr	3.44	4.42	0.57	4.01	4.64	4.90	0.96	4.95	1.84	3.12	1.49	3.39
Co	0.61	0.58	0.96	0.86	0.89	0.84	0.68	0.74	0.59	0.60	0.65	0.59
Zn	3.94	5.01	5.93	3.09	2.94	3.37	0.17	< 0.1	< 0.1	< 0.1	< 0.1	< 0.1
Cu	2.14	2.17	3.59	2.41	2.49	2.61	1.52	1.43	1.31	1.41	1.55	1.48
Sr	4.14	3.52	4.88	3.36	3.29	3.30	1.85	1.79	1.69	2.42	1.64	1.84
Ba	21.6	17.9	17.7	15.7	16.1	16.7	7.34	8.09	7.07	8.54	8.95	6.74
Pb	1.61	1.35	1.46	1.14	1.31	1.40	0.51	0.56	0.55	0.66	0.51	0.54
U	0.06	0.08	0.06	0.03	0.04	0.05	0.02	0.01	0.02	0.02	0.01	0.01

was expected considering roughly half of the SSG and DSG sediment was magnetic, thus implying there is a great amount of detrital magnetite and magnetite-bearing lithic fragments in the sediment. Other iron oxides such as hematite or maghemite may also have dissolved in Step D of the sequential extraction.

Many of the trace elements correlated with iron (Table 15), which reflected the ability of magnetite to incorporate many metals into its crystal structure. The manganese extracted in this step was approximately 10% of the concentrations seen in Step C; however, the relationship between manganese and cobalt was only slightly greater than that seen between the two metals in Step C. The manganese may not have dissolved completely in Step C due to large grain sizes.

Table 15. Cation correlations with iron and manganese determined in Step D of the sequential extraction.

Iron Correlations	r	Slope (mol/mol)	Manganese Correlation	r	Slope (mol/mol)
Al	0.95	1.01×10^{0}	Co	0.58	3.76×10^{-2}
Mg	0.70	7.88×10^{-1}			
Ba	0.96	4.59×10^{-3}			
Zn	0.96†	4.64×10^{-3}			
Sr	0.95	1.45×10^{-3}			
Cu	0.90	1.20×10^{-3}			
Pb	0.95	2.53×10^{-4}			
U	0.89	1.01×10^{-5}			

Critical correlation value for a 10% confidence level with 12 samples is 0.497.

†Critical correlation value for a 10% confidence level with 7 samples is 0.669.

Cations Associated with Organic Matter and Sulfide Minerals

Cations associated with organic matter and sulfides are listed in Table 16. Major elements including calcium and magnesium were prevalent as well as minor and trace elements such as iron, manganese, chromium, and zinc. Sulfur species were not a major component of the ZERT groundwater, neither were sulfide minerals a significant part of the sediment. Results for sulfur and organic carbon concentrations determined by SGS can be found in Table 17. The analysis by SGS showed sulfur concentrations ranging from <0.1 to 0.5 mg/g in residual samples, and <0.1 to 0.4 mg/g in total fractions. With many sulfur concentrations (Table 17) hovering close to the detection limit (0.1 mg/g), it was difficult to determine how much sulfide was in each sample before and after the sequential extraction. It was likely that there were trace amounts of sulfide minerals such

Table 16. Cation concentrations in organic matter and sulfide minerals determined during Step E of the sequential extraction.

Sample	Z-003	Z-015	Z-006	Z-018	Z-019	Z-020	Z-009	Z-024	Z-025	Z-026	Z-012	Z-029
Well	W7	W8	W7	W8	W8	W8	W7	W8	W8	W8	W7	W8
Soil Type	Topsoil	Topsoil	B Hor.	B Hor.	B Hor.	B Hor.	SSG	SSG	SSG	SSG	DSG	DSG
Major Cations (mg/g)												
Ca	0.22	0.27	0.23	0.49	0.52	0.45	0.36	0.50	0.47	0.69	0.39	0.46
Mg	0.50	0.77	0.63	0.62	0.62	0.56	0.23	0.35	0.30	0.34	0.19	0.27
Na	0.05	0.07	0.07	0.15	0.15	0.13	0.11	0.15	0.13	0.13	0.11	0.14
K	0.20	0.32	0.07	0.09	0.09	0.08	0.04	0.05	0.04	0.05	0.03	0.04
Al	1.52	2.08	1.16	1.22	1.27	1.11	0.61	0.75	0.66	0.68	0.60	0.77
Fe	0.42	0.91	0.16	0.25	0.26	0.17	0.07	0.14	0.11	0.08	0.07	0.10
Minor and Trace Cations (µg/g)												
Mn	9.04	14.4	9.25	9.61	9.94	9.96	4.50	7.35	7.91	12.7	4.36	6.89
Li	1.67	2.33	1.43	1.06	1.20	0.97	0.27	0.33	0.34	0.36	0.21	0.31
Cr	4.93	6.32	2.02	1.79	1.64	1.77	0.49	0.82	0.62	0.97	0.69	0.90
Co	0.35	0.66	0.37	0.48	0.48	0.40	0.22	0.38	0.33	0.33	0.19	0.26
Zn	2.37	7.91	2.53	3.28	3.36	2.28	1.18	2.17	2.26	1.54	0.91	1.84
Cu	0.26	0.34	0.30	0.43	0.46	0.28	0.18	0.43	0.32	0.24	0.19	0.23
Sr	2.94	4.10	3.31	5.52	7.56	6.28	4.63	6.48	5.67	7.06	4.66	5.91
Ba	5.45	7.62	4.59	7.59	8.28	7.31	5.24	6.92	7.11	7.10	6.26	6.47
Pb	0.11	0.09	0.10	0.09	0.21	0.17	0.07	0.06	0.06	0.04	0.09	0.05
U	0.15	0.16	0.07	0.06	0.06	0.06	0.02	0.03	0.03	0.03	0.02	0.02

as pyrite in the ZERT soil. Sulfide concentrations in the range of tens of micrograms per gram of soil, far less than the lower detection limit, may have been associated with the tens of micrograms per gram of trace metals in Step E. This means that trace amounts of sulfides could have dissolved even though sulfur was not detected in significant quantities. However, aside from lead and copper, most of the trace metals correlated strongly with organic matter (Table 18), so it is likely that sulfide minerals contributed little to the trace metal concentrations.

Unlike sulfur, organic carbon was present in detectable quantities in the fresh sediment samples (Table 17). As expected, the topsoil had the most organic carbon (16 –

Table 17. Organic carbon and sulfur concentrations in the sediment determined by SGS. Organic carbon, determined with coulometry, was not analyzed for in sediment that underwent the sequential extraction. Sulfur was determined using ICP-MS.

		Organic Carbon Coulometry mg/g	Sulfur ICP-MS mg/g
Extracted Sediments (Step F)			
ZRT-003	topsoil	ND	0.1
ZRT-006	caliche	ND	0.1
ZRT-009	SSG	ND	< 0.1
ZRT-012	DSG	ND	< 0.1
ZRT-015	topsoil	ND	0.5
ZRT-018	caliche	ND	0.3
ZRT-019	caliche	ND	0.1
ZRT-020	caliche	ND	0.2
ZRT-024	SSG	ND	0.1
ZRT-025	SSG	ND	0.1
ZRT-026	SSG	ND	< 0.1
ZRT-029	DSG	ND	0.1
Fresh Sediments (Step T)			
ZRT-001	topsoil	15.6	0.3
ZRT-004	caliche	3	0.2
ZRT-007	SSG	0.7	< 0.1
ZRT-010	DSG	<0.5	< 0.1
ZRT-013	topsoil	29.8	0.4
ZRT-016	caliche	3.8	0.2
ZRT-022	SSG	0.6	< 0.1
ZRT-028	DSG	0.7	< 0.1

30 mg/g), and the sandy gravels had little to none (0.7 – < 0.5 mg/g). The B horizon samples had a moderate amount of organic carbon (3 – 4 mg/g). In addition, the organic matter correlates strongly with many cations including iron, chromium, and uranium (Table 18). The organic carbon content is the amount of organic carbon consumed

during the sequential extraction. This was calculated from the difference between the concentrations of organic carbon in a fresh sediment aliquot and an aliquot that was exposed to the extraction procedure. Since there were only eight fresh sediment aliquots, there were only eight data points used to calculate the correlations. Most of these elements easily adsorb onto organic matter, thus it is reasonable that they are related to soil organic matter concentrations in the sediment.

Table 18. Cation correlations for Step E of the sequential extraction.

Organic Carbon Correlations	r	Slope (mol/mol)
Mg	0.72	7.33×10^{-3}
Fe	0.99	5.80×10^{-3}
K	1.00	3.00×10^{-3}
Li	0.88	1.15×10^{-4}
Mn	0.82	5.48×10^{-5}
Cr	0.97	4.64×10^{-5}
Zn	0.88	3.36×10^{-5}
Co	0.81	2.38×10^{-6}
U	0.94	2.63×10^{-7}

Critical correlation value for a 10% confidence level with 8 samples is 0.622.

Element Distributions

Total distribution graphs for selected elements are useful for understanding the main components in each sediment type. Cation distributions for selected elements are given in the following figures. Each bar in the charts represents 100% of the selected

cation in each sediment sample, determined by summing the concentrations from steps A-F. The total concentration of each element is given at the top of the bar. The bars are divided into sections representing the percent of the total cation concentration that was extracted in a given step (A-F). Essentially, these bar graphs are graphical representations of data given in tables 3 and 4.

Most major cations that are important mineral building elements are discussed. These include calcium, iron, magnesium, and manganese. Most trace metals that were analyzed for during the sequential extraction are discussed; however, arsenic and cadmium are not discussed because they commonly occur below detection limits or occur in unpredictable quantities due to the heterogeneity of the soil.

Calcium

Calcium was an important element for understanding both bulk soil mineralogy and groundwater geochemistry. This is because it occurs in several minerals, such as feldspars, which are abundant but chemically stable in shallow groundwater environments, and calcite, which was also abundant in the aquifer and very chemically reactive. In addition, free calcium ions exchange and adsorb readily onto mineral surfaces and organic compounds. A bar chart representing calcium proportions from the sequential extraction is shown in Figure 4. Topsoil sediment had the lowest concentration of calcium, around 18 mg/g. Most of the calcium extracted was associated with Step F, which included the residual silicate minerals such as various clays, feldspars, and micas. The next largest percentage of calcium in the topsoil was observed in Step A,

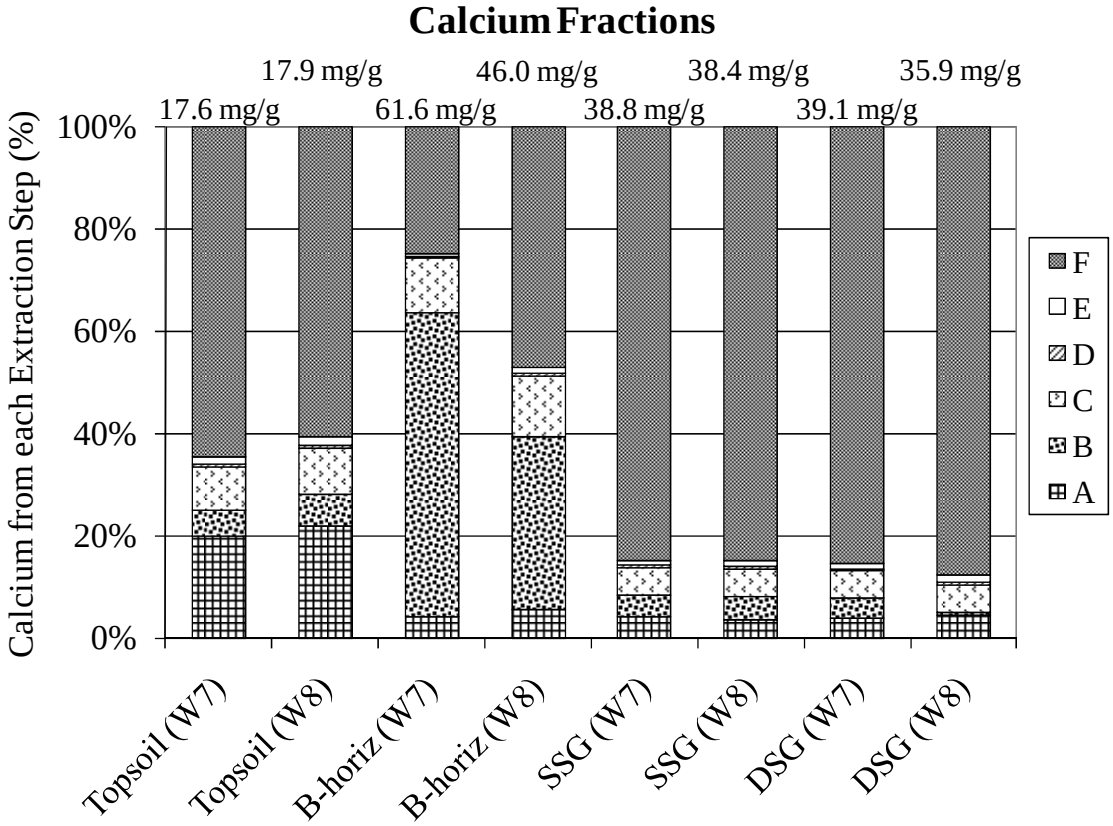

Figure 4. Calcium distribution determined from the sequential extraction.

ion exchange. The high concentration of exchangeable calcium was expected due to the high proportion of clay minerals, which readily adsorb, absorb, and exchange cations. The remainder of the calcium in the topsoil (approximately 15%) was attributed to carbonate, amorphous oxide, and organic phases (B, C, and E, respectively).

The B horizon sediment had the greatest concentration of calcium, 46.0 - 61.6 mg/g. Calcium in the B horizon samples was most abundant in the B and F extraction steps. The B horizon was rich in secondary calcite, which accounted for the 35 – 60% of the total calcium that was found in the B extraction step (Figure 4). Detrital minerals, most likely feldspars, accounted for the large amount of calcium seen in the F step. Five

percent of the calcium was attributed to ion exchange (Step A), which is reasonable because this soil horizon was very fine grained with abundant clay minerals. Finally, 10% of the calcium was observed in Step C and attributed to amorphous oxides. The calcium in this fraction could have been residual dolomite that was not dissolved in Step B, or it could have been calcium oxide inclusions or amorphous calcium oxide globules from weathered minerals.

The sandy gravel samples, SSG and DSG, showed similar calcium distributions and concentrations ranging from 35.9 to 39.1 mg/g. A vast majority of the calcium is found in Step F, which is reasonable due to the high proportion of andesitic, basaltic, and gneissic silicate minerals (including plagioclase feldspar, pyroxenes, and amphiboles) found in this soil horizon. Due to the detrital limestone grains and secondary calcite rims on grains, there is also calcium associated with Step B. Finally, even though the proportion of clays is small compared to other grain sizes, there is still calcium available for ion exchange, Step A, in the sandy-gravel sediment.

Iron

Iron is arguably the second most important element in the ZERT sediment. Iron was equally as abundant as calcium in this sediment, and it occurred in various mineral forms including amorphous oxides, crystalline oxides, and silicate minerals, and it can be associated with organic matter. Figure 5 is a bar chart of the iron fractionation determined by the sequential extraction. It was apparent that most of the iron in all of the ZERT sediment was bound to silicate minerals dissolved in Step F, and thus mostly

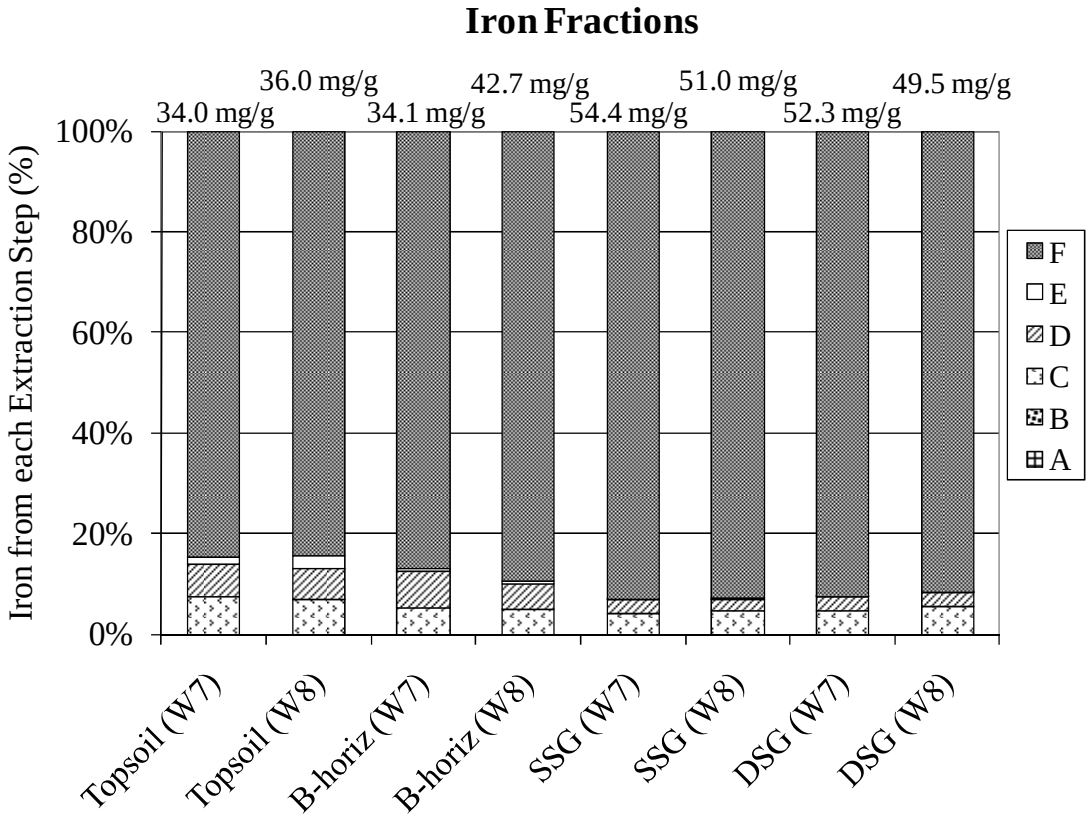

Figure 5. Iron distribution determined from the sequential extraction.

immobile in the groundwater. This is reasonable since a majority of the sediment at the ZERT site is composed of andesitic, basaltic, and gneissic rock fragments, which include a variety of iron silicate minerals. However, the relatively small percentage of iron in non-silicate phases, especially iron in amorphous oxide form (Step C), can account for the increases in iron in the groundwater with the addition of CO_2. Furthermore, iron concentrations in SSG and DSG sediment were slightly higher (49.5 to 54.4 mg/g) than seen in topsoil and B horizon sediment (34.0 to 42.7 mg/g), which can also be attributed to a greater density of iron silicate minerals in the sandy gravel compared to the topsoil and B horizon. Amorphous (Step C) and crystalline (Step D) iron oxides were the second

and third most iron-rich phases in the sediment, likely due to secondary iron oxides and the abundance of magnetite. Finally, the topsoil and B horizon samples contained iron associated with organic matter (Step E).

Magnesium

Magnesium is commonly associated with carbonate minerals, andesitic minerals, and ion exchange, thus it was an important major element in the ZERT system. A bar chart of magnesium proportions determined in the sequential extraction of the ZERT sediment can be found in Figure 6. Topsoil had the lowest concentrations of magnesium (9.5 to 11.1 mg/g), sandy gravel samples had a moderate amount of magnesium (15.5 to 16.4 mg/g), and the B horizon samples had the greatest concentration of magnesium (18.2 to 18.7 mg/g). All samples were dominated by magnesium that was associated with Step F, residual silicate minerals. In the topsoil, the remainder of the magnesium was divided almost equally between ion exchange (Step A) and in amorphous oxide (Step C), crystalline oxide (Step D), and organic (Step E) phases. In B horizon sediment, magnesium not attributed to Step F was common in steps B and C, which was likely due to the high proportion of carbonate minerals in the sediment.

For SSG and DSG samples, magnesium was most abundant in Step C. Some of this magnesium was likely from dolomite dissolution, especially in the sandy gravel where detrital dolomite has been found. Finally, basalt grains in SSG and DSG samples may account for the magnesium fractions seen in steps C and D. Olivine in the basalt in source rocks may have altered to periclase (MgO) before sediment deposition, or brucite

($Mg(OH)_2$) after deposition, both of which are sources of magnesium. According to Deer et al. (1978), brucite and periclase are soluble in HCl, so it is possible that they would dissolve in the strongly acidic conditions of Step D.

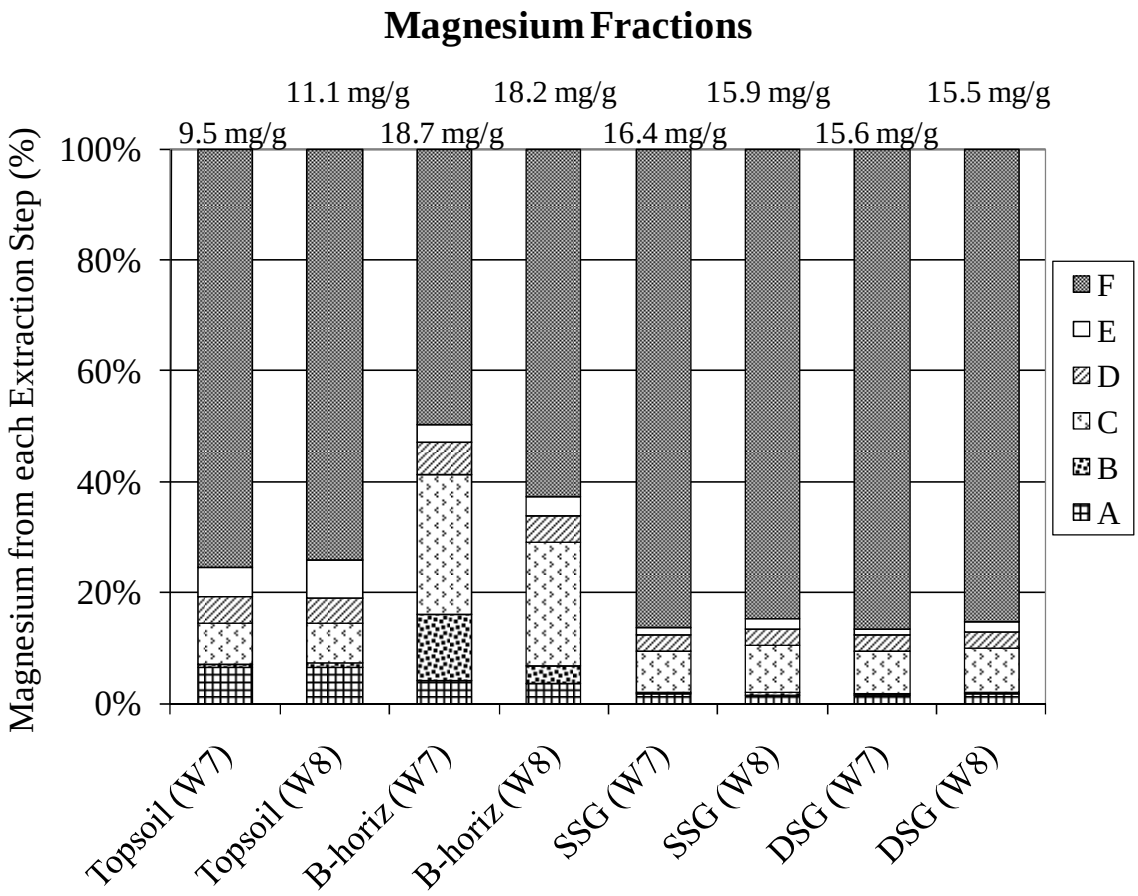

Figure 6. Magnesium distribution determined from the sequential extraction.

Manganese

Manganese was a minor metal in abundance, but of significant interest because manganese oxides are typically heavy metal sinks, and they can incorporate Fe, Zn, Pb, and Co (McKenzie, 1972; Chao and Theobald, 1976). A bar chart of the soil manganese

fractions can be found in Figure 7. Manganese oxides were a minor soil component by concentration; however, they typically occur in poorly crystalline forms with various valence states, and dissolution of manganese oxides in the groundwater has the potential to release these metals into the drinking water supply. Therefore, manganese oxides were a target in the sequential extraction. The concentration of manganese in the ZERT samples ranges from 0.63 to 1.05 mg/g, which was far less than those of calcium, iron,

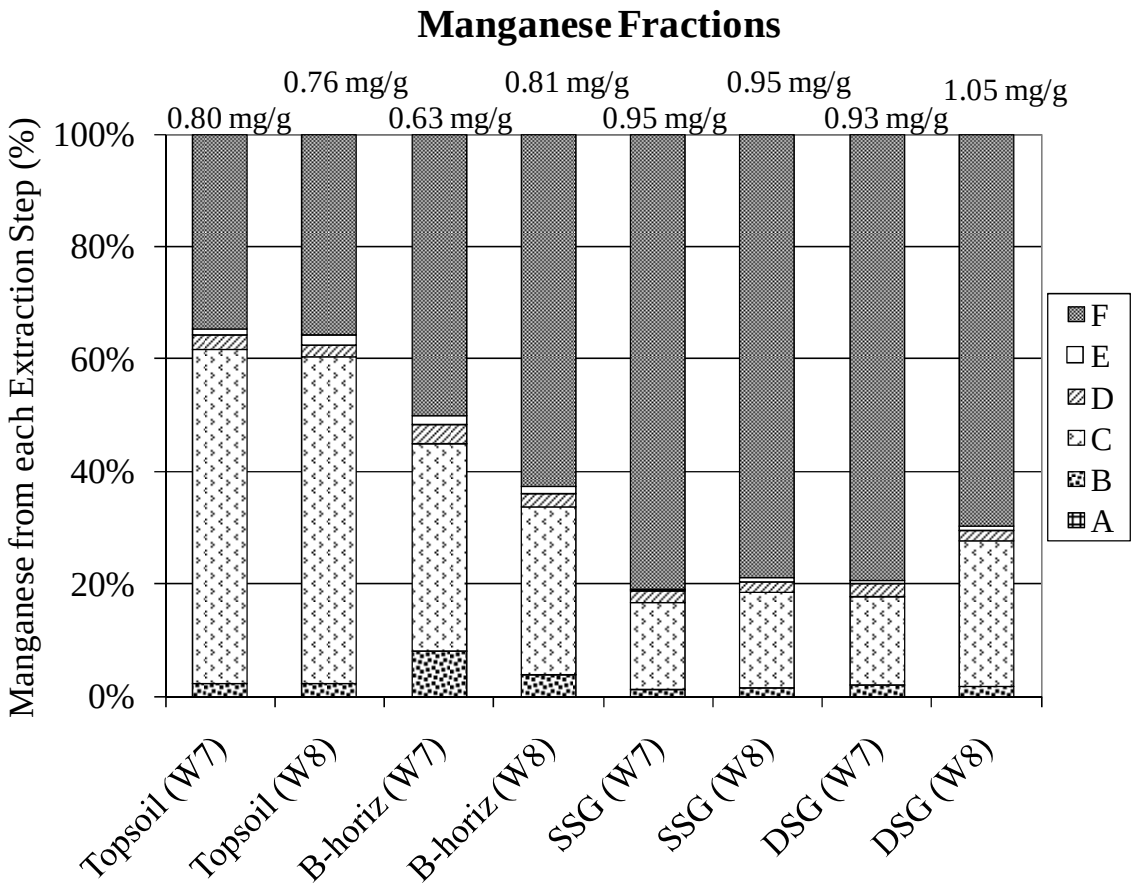

Figure 7. Manganese distribution determined from the sequential extraction.

and magnesium. It was not surprising that a large quantity of the manganese in the ZERT sediment was extracted in Step C, with a majority of the remainder of the manganese occurring in Step F. Manganese oxides are most common in topsoil and B horizon sediment, which are less likely to be in contact with groundwater during the summer. In addition, small quantities are associated with Step B; manganese is a common minor element associated with limestone.

Copper

Copper was of interest because it is regulated in drinking water by the U.S. EPA. A comparison of copper concentrations among the ZERT sediment is shown in Figure 8. Copper is typically chalchophilic, meaning it most often forms bonds with sulfur rather than oxygen. However, very little copper was associated with the sulfides extracted in Step E, which was consistent with the low sulfide concentrations in the ZERT soils. There was very little copper in the soils, with typical concentrations ranging from 24.0 to 33.7 μg/g of soil. Aside from silicate phases (Step F), a majority of the copper was extracted in Step C. This indicated the presence of copper oxides, or much more likely the incorporation of copper into amorphous iron oxide and manganese oxide compounds. Sandy gravel samples had small amounts of copper, around 5%, extracted during Step B; however, copper did not share a linear relationship with calcium so it is unlikely that the copper was released as a result of carbonate dissolution.

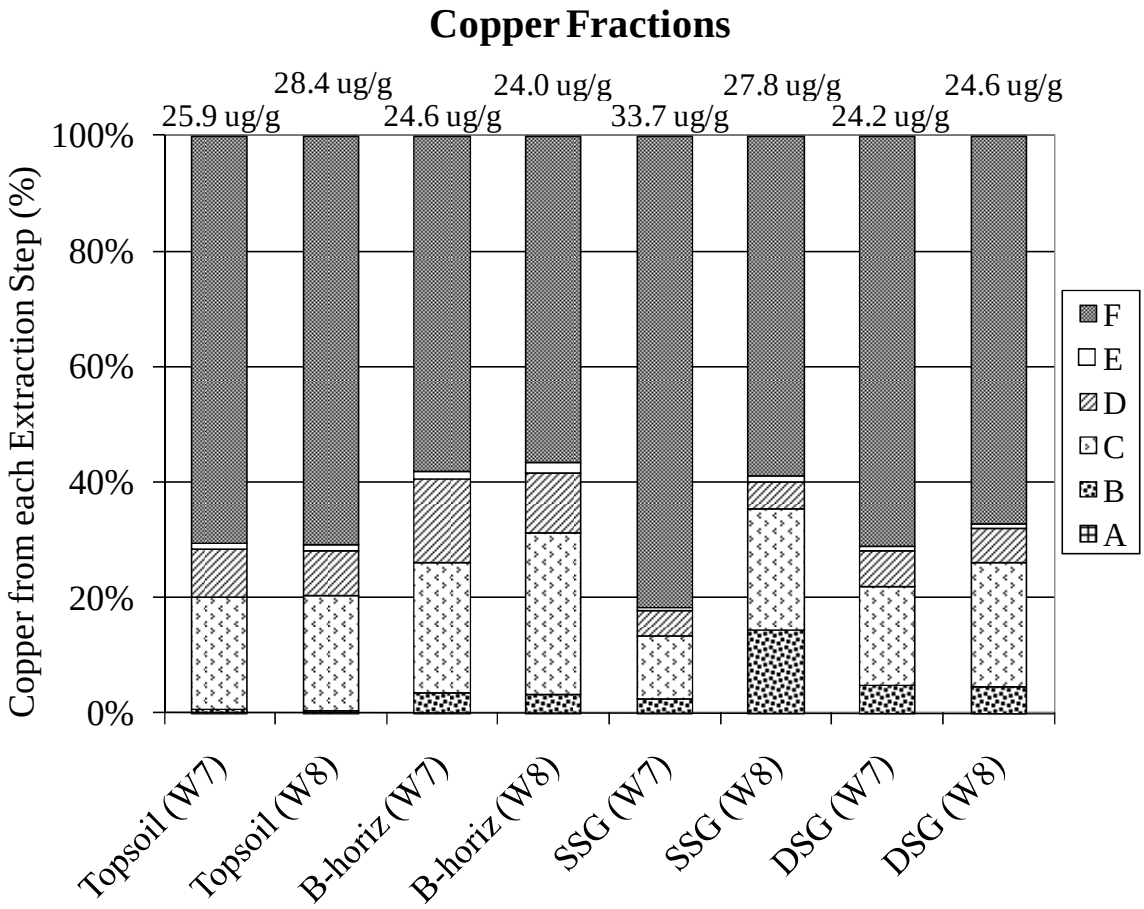

Figure 8. Copper distribution determined from the sequential extraction.

Zinc

Concentration distributions of zinc, another chalcophile element, can be found in Figure 9. Zinc occurs in concentrations ranging from 72 to 97 ug/g for all ZERT samples. Zinc was not liberated to a great extent during the sequential extraction, which is evidenced by the fact that most of the zinc resides in the F fraction for all soil types. Zinc was also consistently found in small amounts in steps C, D, and E. It is probable that most of the zinc in Step E was associated with organic matter rather than sulfides,

due to the strong correlation between zinc and organic carbon concentration (Table 18). Another possibility is the presence of hemimorphite, a secondary, hydrous zinc silicate, and zinc inclusions in amorphous oxides are the feasible zinc sources in Steps C and D. The U.S. EPA (2009) lists zinc as a secondary contaminant of interest in drinking water, and suggests that the concentration of zinc be less than 5 mg/L. Thus, zinc is not hazardous to health, but of interest for aesthetic water quality.

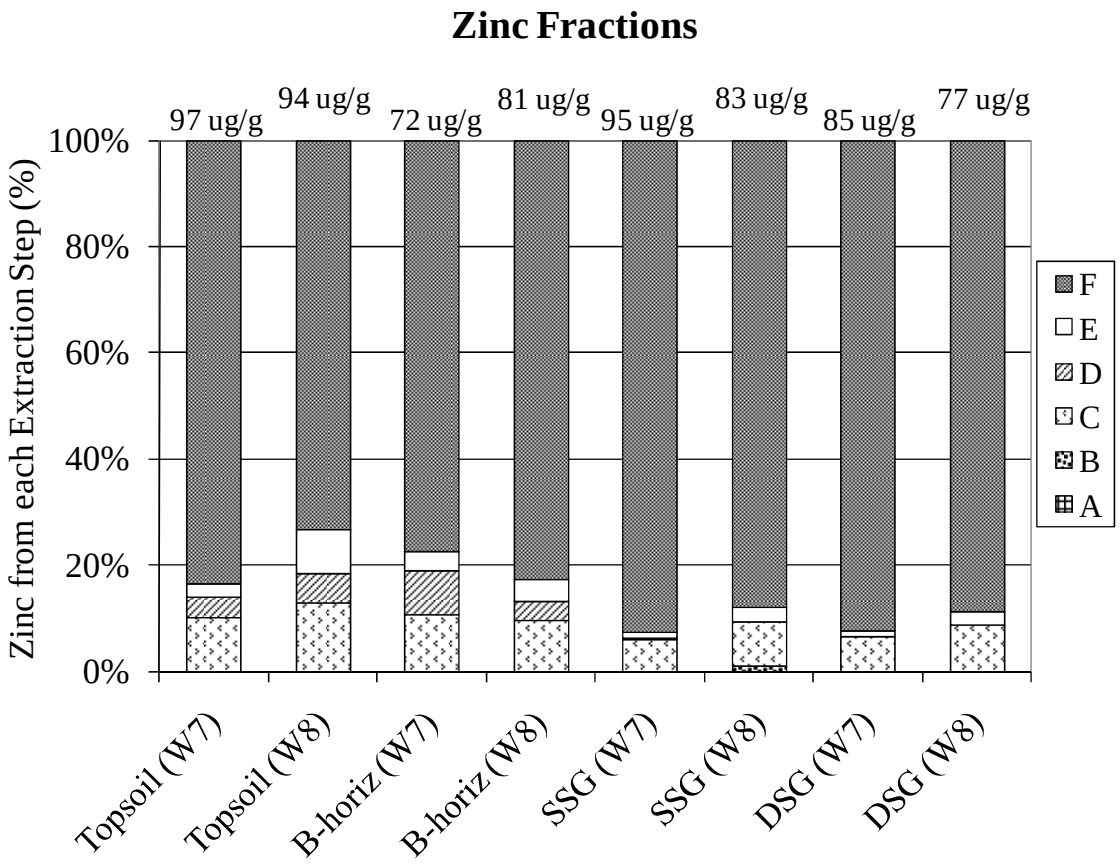

Figure 9. Zinc distribution determined from the sequential extraction.

Lead

Lead in the groundwater is also regulated by the U.S. EPA, with an enforced action level of 0.015 mg/L. A bar chart of the distribution of lead in the ZERT soil can be found in Figure 10. Lead had a fairly uniform distribution in the sediment, with concentrations between 19.7 and 30.5 ug/g. For topsoil and B horizon samples, 40 to 55% of the lead was liberated by the sequential extraction while the remaining 45 to 60% was tied up in silicate minerals (Step F). In addition, the lead that was extracted was

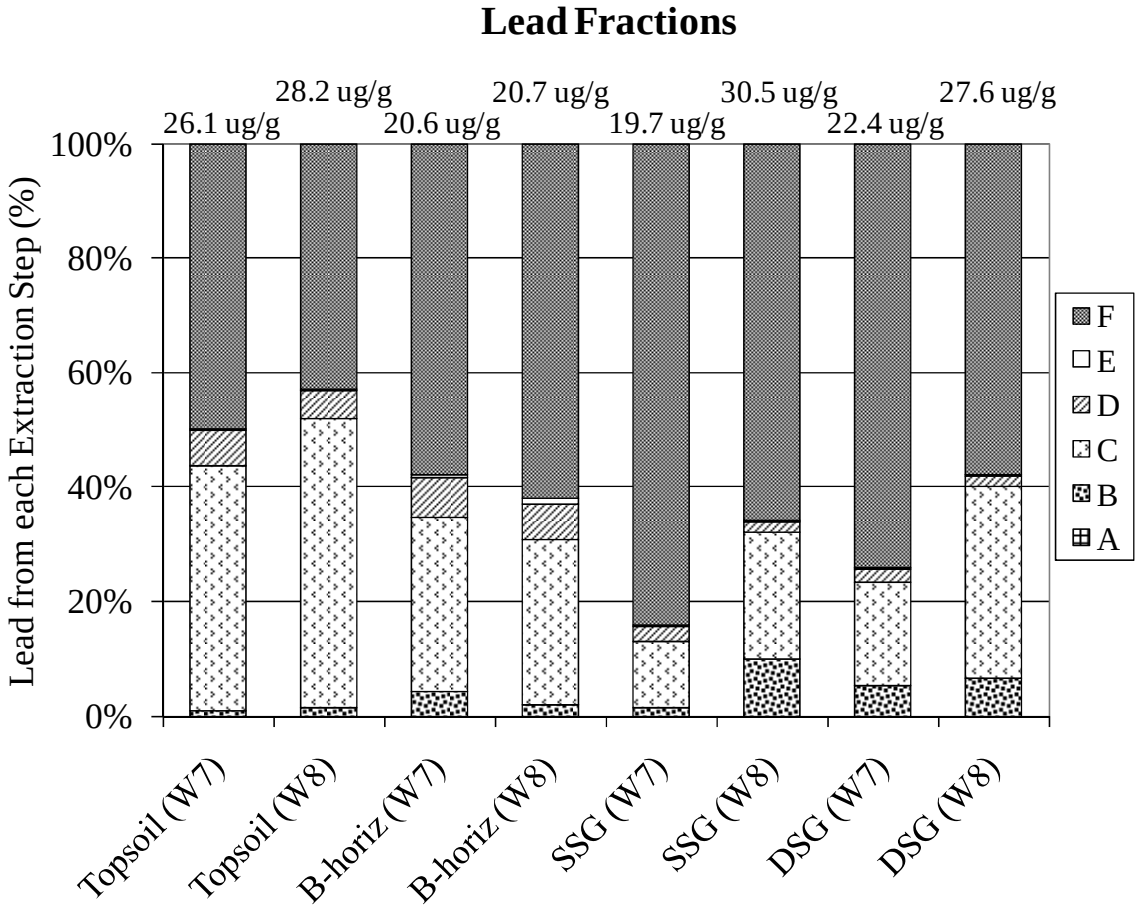

Figure 10. Lead fractions determined from the sequential extraction.

found mostly in steps C and D, and lead concentrations correlated with manganese and iron (tables 12 and 15, respectively), thus implying that lead was present in small amounts in oxide minerals. Finally, there was some lead in Step B samples. Because lead was not correlated with calcium, it is unlikely that the lead was part of the limestone. However, replacement of calcite by lead cations in carbonate crystals may have occurred in situ and could account for lead that did not necessarily correlate with calcium. Or, other lead-bearing minerals may have been present in trace amounts and could have dissolved during Step B, which released lead cations.

Chromium

Chromium was a metal of interest because it has a low MCL in drinking water (0.1 mg/L), and it occurred in significant quantities in the soil (60 to 90 ug/g). A bar chart of the chromium fractions is shown in Figure 11. For all samples, a majority of the chromium was determined to be in Step F, and thus was unaffected by the sequential extraction. About half of the remaining chromium in the topsoil samples was found in Step E, and it was strongly correlated with organic carbon content (Table 18). Otherwise, chromium was associated with oxide minerals, steps C and D. B horizon and sandy gravel samples had a much smaller percentage of chromium associated with organic matter, which was likely due to the lower concentration of organic matter in the sediment. In addition, less chromium was extracted during other steps in the sequential extraction.

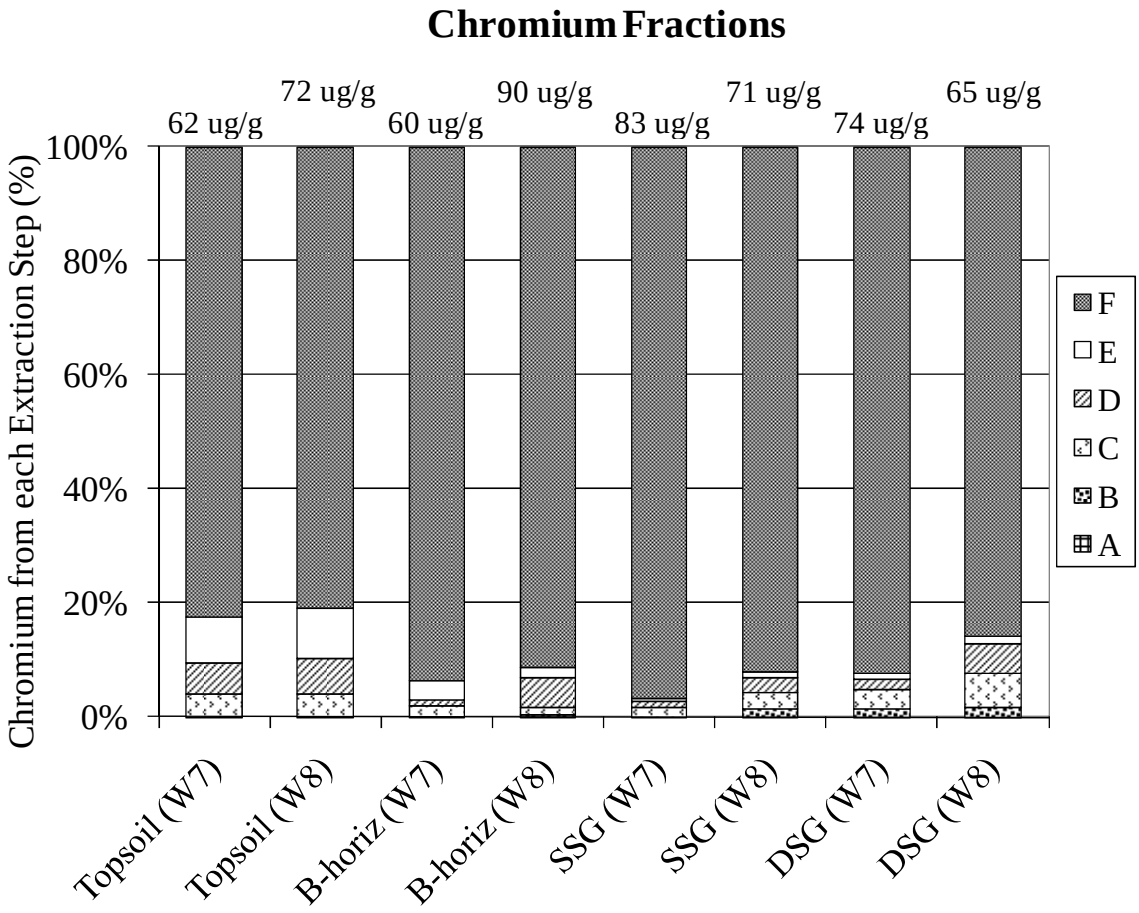

Figure 11. Chromium fractions determined from the sequential extraction.

Barium

Barium, another primary drinking water contaminant regulated by the U.S. EPA, has a higher MCL, 2 mg/L, than other trace elements, which implies it is slightly less toxic than other regulated constituents. However, barium also occurred in greater concentrations in the ZERT sediment than other trace elements. This could mean that extensive dissolution of barium-bearing minerals as a result of CO_2 in the groundwater could cause Ba to exceed allowable barium concentrations in the groundwater. A bar

chart of the barium distribution is shown in Figure 12. Barium occurred in the samples in concentrations ranging from 863 to 1,617 ug/g, and 80 to 95% of this was tightly bound in residual minerals (Step F). Residual mineral dissolution poses little risk to groundwater contamination. The remaining barium was closely associated with ion exchange (A), carbonates (B), and manganese oxides (C).

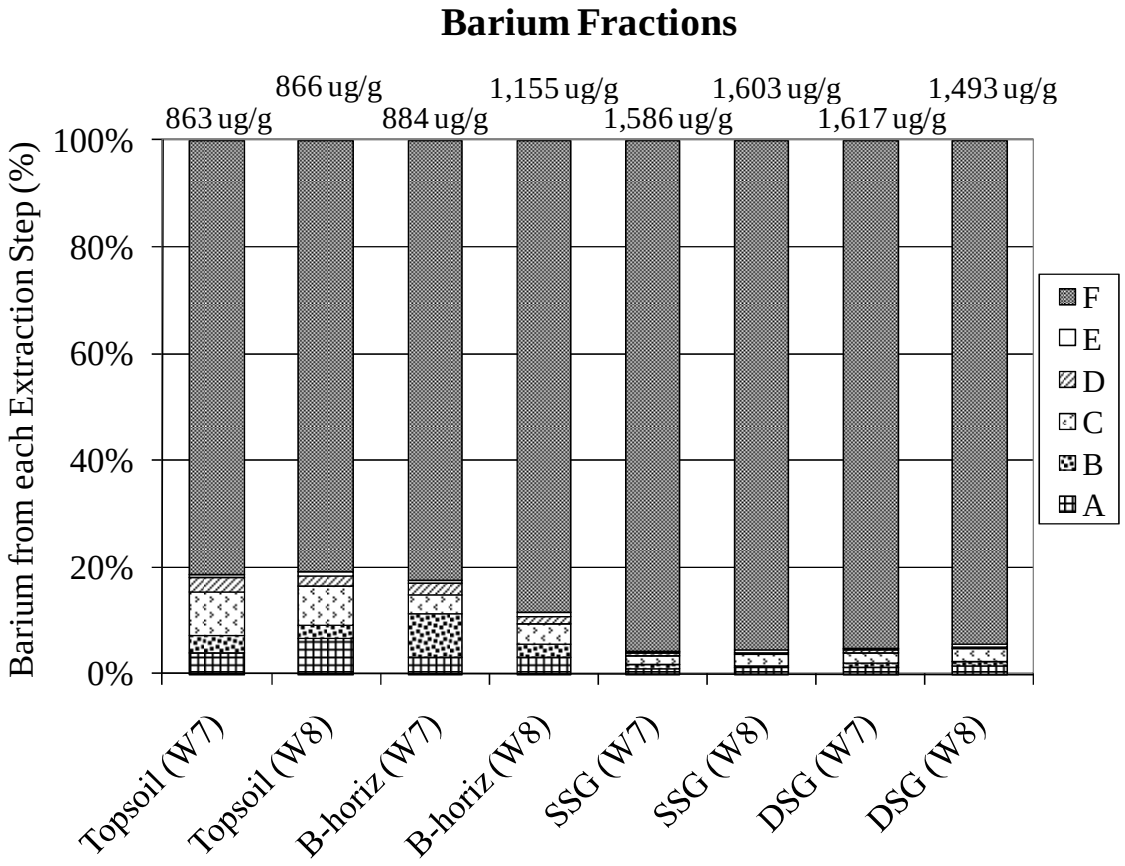

Figure 12. Barium distribution determined from the sequential extraction.

Carbonates Dissolved in Step A

Some of the exchangeable cations from Step A, including calcium, magnesium, and strontium, are also typically associated with carbonate dissolution. Therefore, it was hypothesized that a fraction of carbonate minerals, especially the fine-grained, secondary carbonate coatings, were dissolved during Step A, which would inflate the exchangeable cation concentrations determined. If 5% of the carbonate dissolved, an arbitrarily chosen value, the effects on the cation concentrations for the topsoil and sandy gravel would be moderate, but there could be substantial changes to the cation concentrations in the B horizon samples because they contain more carbonate by mass. Furthermore, it was assumed that exchange occurs rapidly, where as carbonate dissolution would continue with time.

To test this, Step A was repeated with fresh sediment splits; three from W8 B horizon, three from W8 shallow sandy gravel, and three from W8 deep sandy gravel. The sediment was shaken in 1.0 M cesium chloride for either 15, 30, or 60 minutes. Following this, the sediment slurries were centrifuged, and the liquid extractants were decanted. An aliquot of each of the resulting extractants was acidified for analysis by ICP-MS, while the remaining solution was titrated for alkalinity using 0.01 N sulfuric acid. The ICP-MS results are listed in Table 19. In addition to cation concentrations, Table 19 also lists the CEC values for each sample. The cation concentrations and the CEC values were in agreement with the original samples (Table 7). Therefore, it was reasonable to assume that the sediment aliquots were representative.

Table 19. Cation concentrations resulting from the CsCl extraction redo.

Sample	Z-107	Z-106	Z-017	Z-023	Z-111	Z-110	Z-114	Z-115	Z-030
Well	W8	W8	W8	W8	W8	W8	W8	W8	W8
Soil Type	B Hor.	B Hor.	B Hor.	SSG	SSG	SSG	DSG	DSG	DSG
Ext. Time (min)	15	30	60	15	30	60	15	30	60
Major and Minor Cations (mg/g)									
Ca	2.1	2.0	1.8	1.0	1.0	1.2	1.0	1.2	1.3
Mg	0.57	0.55	0.50	0.17	0.18	0.20	0.19	0.22	0.22
K	0.11	0.11	0.11	0.13	0.14	0.15	0.14	0.14	0.14
Na	0.022	0.022	0.020	0.013	0.013	0.015	0.017	0.024	0.022
Sr	0.009	0.009	0.008	0.004	0.004	0.004	0.004	0.005	0.004
Ba	0.025	0.025	0.024	0.011	0.012	0.013	0.016	0.019	0.019
CEC (meq/100g)									
	15.5	15.2	13.8	6.9	7.0	7.8	7.0	8.4	8.9

The pH and titration results for each sample are shown in Table 20. It is known that cation exchange rates increase for decreasing grain size. According to Malcolm and Kennedy (1970), exchange reactions for clay and silt particles are typically completed within 100 seconds, while it takes 20 minutes to an hour for larger sand particles. Since the ZERT samples were a mixture of grain sizes and the cation concentrations did not increase with time, it was concluded that the exchange reactions were completed after 15 minutes. Furthermore, if dissolution of calcite was occurring, it either ceased before 15 minutes, or the rate was too slow to be determined within an hour.

It was evident with the change in pH and the increase in alkalinity in all samples that a fraction of the carbonate dissolved during Step A. In addition, more carbonate dissolved in the B horizon samples than the sandy gravel samples, which accounted for the greater alkalinity. This was expected because of the higher concentration of carbonate minerals in the B horizon. However, the increases in pH from 5.2 to close to 8,

and alkalinity from 0 mg/L as HCO_3^- to lower 30s for sandy gravels and 50s for B horizons samples were not strongly time dependant, which suggested that the carbonate in the samples dissolved quickly. The undetermined (ND) value for alkalinity for sample Z-111 resulted because the sample was not properly titrated so the datum was lost. Therefore, the amount of calcium from carbonate could not be estimated for this sample.

Table 20. Alkalinity and pH changes resulting from the CsCl extraction redo. "Reg Blk" is the cesium chloride reagent blank for these batch extractions.

Sample	Soil Type	Ext. Time (min)	pH	Alkalinity (mg/L as $HCO3^-$)	Ca from Carbonate (mg/g)
Reg Blk	1 M CsCl		5.2	0.0	0
Z-107	W8 B Hor.	15	7.8	51.7	0.129
Z-106	W8 B Hor.	30	7.3	50.5	0.126
Z-017	W8 B Hor.	60	8.0	59.4	0.152
Z-023	W8 SSG	15	7.7	34.1	0.085
Z-111	W8 SSG	30	7.6	ND	ND
Z-110	W8 SSG	60	8.1	31.7	0.081
Z-114	W8 DSG	15	7.8	27.2	0.068
Z-115	W8 DSG	30	7.3	31.9	0.082
Z-030	W8 DSG	60	8.0	35.0	0.088

The slight increases in alkalinity that are there after 15 minutes were attributed to the heterogeneity of the sediment aliquots. The rapid dissolution of carbonates was likely due to the very small grain size of the carbonates. In addition, some of the bicarbonate ions in the solution could be from anion exchange with chlorine in the 1.0 M CsCl reagent. Table 20 also lists calculated calcium concentrations that would have resulted from the dissolution of carbonate, which yielded the observed alkalinity. These values

were on average 7% of the total calcium concentrations for the samples listed in Table 19. Thus, a majority of the calcium and other cations in the cesium chloride extractions were a result of cation exchange.

DISCUSSION

Groundwater Chemistry

The main objective of this study was to compare the soil chemistry determined with the sequential extraction procedure with the groundwater chemistry to define the sources of metals in the groundwater with the addition of CO_2. Changes in groundwater chemistry, specifically changes in dissolved cation concentrations, as a result of carbon dioxide injection at the ZERT site in 2008 and 2009 were measured using ICP-MS.

Though many wells were sampled, this analysis focused on wells 2B and 5B (Figure 2) due to their similar proximities to the CO_2 source, which translates to similar response times to CO_2 injection. Both wells were within 2 m of the horizontal CO_2 injection pipeline. The focus was further narrowed to the changes in water chemistry that occurred up to seven days after CO_2 injection. In 2008, groundwater was analyzed for the entire injection duration; however, episodes of rainfall disrupted the system at several times starting seven days after the injection began. The data after rainfall add uncertainty and complexity to the analysis at hand, so only the first seven days of samples plus three days of background samples were considered in the analysis (July 7 to July 17, 2008, with CO_2 injection starting July 11, 2008). In 2009, groundwater was sampled for only six days after injection started with two days of sampling beforehand, so the data set is limited in time. All eight days worth of 2009 data were considered in the analysis (July 13 to July 21, 2009, with CO_2 injection starting July 15, 2009).

Tables 21 and 22 show the ZERT groundwater chemistry before and during injection of CO_2. Table 21 shows the background water chemistry from the ZERT site before injection of CO_2 in 2008 and 2009. Data from 2008 was reported by Kharaka et al. (2010), and data from 2009 is unpublished. The sampling wells are shown on the map in Figure 2. Before injection, the groundwater had a pH between 6.6 and 7.0, with a low range of alkalinities between 305 and 434 mg/L as HCO_3^-. Calcium was the dominant cation with concentrations between 62 and 92 mg/L. Background magnesium concentrations ranged from 19 to 28 mg/L, and iron concentrations were below detection limits in all but one background sample. Finally, manganese ranged from 0.07 ug/L to 0.31 mg/L in background water samples.

Table 22 shows the ZERT groundwater chemistry for the first few days following the start of the CO_2 injection for wells 2B and 5B in 2008 and 2009. Similar to Table 21, data from 2008 was reported by Kharaka et al. (2010), and data from 2009 is unpublished. Following the injection, the pH dropped to values between 5.8 and 6.4, while alkalinities increased to values between 664 and 1,174 mg/L as HCO_3^-. In addition, there were marked increases in the concentrations of calcium (137 to 204 mg/L), magnesium (41 to 70 mg/L), iron (0.01 to 0.93 mg/L), and manganese (0.0008 to 0.19 mg/L) during the injection of CO_2. During the injection, some trace element concentrations increased linearly with alkalinity. These elements included Sr, Ba, Al, Li, Cu, Cd, and Cr, and to a lesser degree U, and Pb.

Table 21. Background ZERT groundwater geochemistry data from 2008 and 2009 before the injection of CO_2 (2008 data published in Kharaka et al., 2010; 2009 data unpublished).

Sample	08-104	08-105	08-106	08-107	08-109	09-101	09-102	09-103	09-104	09-105	09-106	09-107	09-108
Well	4B	1A	4A	2A	2B	3B	1B	2B	5B	4B	W8	W6	W7
Date	7/7/08	7/8/08	7/8/08	7/8/08	7/9/08	7/13/09	7/14/09	7/14/09	7/14/09	7/14/09	7/15/09	7/15/09	7/15/09
pH	6.9	6.9	6.9	6.7	7.0	6.7	6.6	6.6	6.6	6.7	6.6	6.7	6.8
Alkalinity (mg/L)	431	386	398	387	434	336	364	349	352	336	366	318	305
Major and Minor Cations (mg/L)													
Ca	90	84	86	84	92	92	75	71	69	69	78	65	62
Mg	27	23	25	24	28	28	21	21	23	20	22	19	19
Na	9.7	7.8	8.1	7.5	9.1	9.1	8.1	8.5	8.8	8.3	8.1	7.7	7.4
K	5.6	5.6	5.6	5.3	5.4	5.4	5.3	4.7	4.1	4.9	5.5	5.2	5.0
Mn	0.11	0.001	0.31	0.001	0.028	0.028	0.00009	0.00007	0.00015	0.009	0.003	0.046	0.046
Fe	0.05	<0.01	<0.01	<0.01	<0.01	<0.01	<0.01	<0.01	<0.01	<0.01	<0.01	<0.01	<0.01
Sr	0.30	0.27	0.28	0.26	0.30	0.30	0.24	0.23	0.25	0.23	0.25	0.21	0.20
Ba	0.10	0.11	0.10	0.11	0.10	0.10	0.09	0.08	0.08	0.08	0.10	0.09	0.08
Trace Cations (µg/L)													
Al	3	2	2	3	3	3	1	1	<1	1	1	1	1
Li	0.006	0.003	0.004	0.005	0.007	0.007	0.0032	0.0039	0.0042	0.0035	0.0031	0.0026	0.0025
Co	0.8	<0.2	0.6	0.2	0.4	0.4	<0.2	<0.2	<0.2	<0.2	<0.2	0.3	<0.2
Cu	2.4	1.2	1.1	1.6	2.5	2.5	1.4	1.6	2.0	1.6	1.4	1.4	1.5
Zn	2.4	2.8	3.2	3.1	3.8	3.8	2.2	1.4	2.9	3.3	2.5	6.6	1.9
Cd	0.26	0.08	0.10	0.23	0.29	0.29	<0.04	<0.04	<0.04	<0.04	0.04	<0.04	<0.04
Pb	0.08	0.02	0.02	0.05	0.06	0.06	<0.02	<0.02	<0.02	<0.02	<0.02	<0.02	<0.02
Cr	10	<0.4	<0.4	12	12	12	1.9	1.3	2.3	2.1	1.8	1.7	1.7
U	4.5	4.0	4.0	4.1	4.3	4.3	3.6	3.2	3.1	3.3	3.8	3.1	3.1

Table 22. ZERT groundwater geochemistry data from 2008 and 2009 during the injection of CO_2. (2008 data published in Kharaka et al., 2010; 2009 data unpublished).

Sample	08-116	08-124	08-129	08-133	08-118	08-128	08-132	09-110	09-116	09-111	09-119
Well	5B	5B	5B	5B	2B	2B	2B	2B	2B	5B	5B
Date	7/11/08	7/14/08	7/15/08	7/17/08	7/12/08	7/15/08	7/17/08	7/17/09	7/21/09	7/17/09	7/21/09
pH	6.2	6.0	6.0	5.9	6.4	5.9	5.9	5.8	5.8	6.1	6.1
Alkalinity (mg/L)	994	1174	982	1060	664	816	924	900	814	665	811
Major and Minor Cations (mg/L)											
Ca	190	201	181	199	142	204	191	189	184	137	174
Mg	66	68	64	70	41	54	49	51	45	42	50
Na	12.7	11.7	11.3	11.2	9.7	10.1	9.5	10.7	9.2	11.1	10.3
K	6.5	6.8	6.8	6.8	7.1	8.3	8.0	7.3	7.0	5.7	6.6
Mn	0.046	0.14	0.17	0.19	0.19	0.13	0.14	0.006	0.012	0.0008	0.002
Fe	0.19	0.63	0.93	0.72	0.08	0.39	0.53	<0.02	<0.028	<0.01	<0.018
Sr	0.67	0.71	0.63	0.71	0.45	0.63	0.57	0.58	0.55	0.47	0.58
Ba	0.25	0.27	0.26	0.27	0.19	0.27	0.26	0.23	0.21	0.16	0.22
Trace Cations (µg/L)											
Al	8	8	7	7	5	7	6	4	7	1	<1.9
Li	0.011	0.013	0.012	0.010	0.008	0.010	0.007	0.0066	0.0058	0.0053	0.0068
Co	1.0	2.5	3.1	2.4	1.2	1.2	1.2	<0.4	<0.4	<0.3	<0.3
Cu	2.7	2.8	2.4	2.3	2.3	2.6	2.2	1.8	1.8	2.2	2.2
Zn	3.9	5.9	3.6	4.2	9.0	3.2	2.3	12.6	3.8	6.1	5.2
Cd	0.41	0.59	0.56	0.58	0.45	0.61	0.43	<0.08	<0.08	<0.05	0.06
Pb	0.07	0.10	0.08	0.09	0.08	0.10	0.06	<0.04	<0.04	<0.03	<0.03
Cr	46	87	76	20	54	72	21	9.3	9.6	5.3	12.6
U	4.7	4.9	4.7	5.2	3.8	4.5	4.3	1.7	1.9	3.5	2.5

Geochemical Modeling of the Groundwater

Two modeling applications were used to model groundwater chemistry, PHREEQC, and SOLMINEQ. Saturation indices were modeled using PHREEQC Version 2.17.5, which is written and maintained by David Parkhurst at the U.S. Geological Survey (Parkhurst and Appelo, 1999). SOLMINEQ was used to model dissolution of carbonate phases with various partial pressures of carbon dioxide (P_{CO2}). SOLMINEQ was written by Kharaka et al. (1988).

PHREEQC has a variety of groundwater chemistry applications; however, only speciation and saturation index (SI) calculations were used to assess the water-rock interactions in the ZERT aquifer with the addition of CO_2. It is important to note that negative SI values typically indicate solutions that are undersaturated with respect to dissolving minerals, and positive SI values represent supersaturation. Supersaturation of solution with respect to a mineral does not necessarily mean that the mineral is precipitating; some precipitation reactions are extremely slow, thus keeping the water supersaturated for long lengths of time (Deutsch, 1997). Finally, SI values for reactive minerals within a range of 0 ± 0.5 represent minerals that control groundwater chemistry (Deutsch, 1997). Results for the ZERT groundwater can be found in Table 23. Before injection of CO_2, the groundwater was undersaturated with respect to carbonate minerals. The saturation indices for carbonate minerals did not change significantly with the addition of CO_2. It is likely that calcite strongly influences the background water

Table 23. Saturation indices for select minerals in the ZERT groundwater both before and during CO_2 injection, calculated using PHREEQC. Negative values indicate undersaturated minerals, and positive values indicate supersaturation.

		Saturation Index	
Mineral	**Formula**	**Background**	**With CO_2**
Carbonates			
Calcite	$CaCO_3$	-0.28	-0.55
Dolomite	$CaMg(CO_3)_2$	-0.93	-1.50
Rhodochrosite	$MnCO_3$	-1.86	-1.37
Siderite	$FeCO_3$	-11.06	-9.31
Smithsonite	$ZnCO_3$	-3.77	-4.30
Strontianite	$SrCO_3$	-2.25	-2.48
Witherite	$BaCO_3$	-3.51	-3.71
Oxides			
Goethite	FeO(OH)	6.77	7.54
Hausmannite	$Mn^{2+}Mn^{3+}{}_2O_4$	-0.62	-2.75
Hematite	Fe_2O_3	15.50	17.01
Manganite	MnO(OH)	3.14	2.86
Pyrolusite	MnO_2	6.94	6.37
Pyrochroite	$Mn(OH)_2$	-8.60	-9.21
Iron Hydroxide	$Fe(OH)_3$	1.33	2.24

chemistry because it is considered a reactive mineral and its SI value is -0.28, which is within the error bounds typically accepted for equilibrium (0 ± 0.5), as described above. With the addition of CO_2, the saturation index decreases, which indicates calcite still has the potential to dissolve.

Saturation indices for iron and manganese oxides other than hausmannite also did not change significantly with the injection of CO_2 in the groundwater. The manganese oxides hausmannite and pyrochroite had negative SI values, indicating they were either dissolving or were not present in the aquifer. Pyrochroite easily oxidizes (Albering,

1999), so it is likely not present in the shallow ZERT aquifer. Hausmannite is a rare manganese ore with supergene origins, and it is unlikely to occur in large quantities in the alluvial environment that is the setting for ZERT (Hewett, 1972). The groundwater was supersaturated with respect to other iron and manganese oxides, so it is evident that dissolution of these minerals did not affect the groundwater chemistry.

SOLMINEQ was initially used to determine anticipated pH as a result of CO_2 injection into the ZERT aquifer, assuming there was no interaction with carbonate minerals. When CO_2 was injected into water, some of the CO_2 dissolved and formed carbonic acid (1). The dissociation of this acid released hydrogen ions into the water (2), thus decreasing the pH, which caused the dissolution of calcite.

$$H_2O + CO_2 \leftrightharpoons H_2CO_3 \qquad (1)$$

$$H_2CO_3 \leftrightharpoons H^+ + HCO_3^- \qquad (2)$$

For this model, a representative background sample (08-109) was chosen. The sample was subjected to increasing model P_{CO2} values without equilibrating with calcite. If the pH of the model resembled the observed pH, it was assumed that calcite and other carbonates are not dissolving. However, if the modeled pH was lower than observed values, it was inferred that carbonate minerals were dissolving in the aquifer during CO_2 injection, with dissolution consuming hydrogen ions and raising the pH higher than if carbonate minerals were not dissolving. The background value of P_{CO2} was < 0.05 bars, and the maximum P_{CO2} was set to 1.1 bars. Bozeman, MT, has a typical summer atmospheric pressure of 1 atm, or 1.013 bars. A few meters under the surface, the pressure could be slightly greater than 1 atm. Furthermore, monitoring of vadose gases

showed that some locations almost reached complete saturation with CO_2 during the injection (unpublished data). Thus, a maximum of 1.1 bars of CO_2 is acceptable. The results are shown in Table 24 under the "pH without equilibrating with calcite" column. At high P_{CO2}, the predicted pH was 5.54 to 5.63, which is below the minimum observed pH of 5.8. Thus, it was inferred that calcite or other carbonates were dissolving. This is in agreement with the PHREEQC model results, which indicate that the water was undersaturated with respect to calcite during the injection of CO_2.

Also shown in Table 24 are results from simulations that incrementally increase P_{CO2} while dissolving calcite to saturation; included are pH, alkalinity, and calcium concentrations from these simulations as well as the amount of calcite dissolved. The pH

Table 24. Results from SOLMINEQ simulations of increasing P_{CO2} in a background ZERT groundwater sample.

P_{CO2} (bar)	CO_2 (mol/kg water)	pH without equilibrating with calcite	pH with calcite saturation	Calcite needed to reach saturation (mol/kg water)	Alkalinity (mg/L as HCO3)	Calcium (mg/L)
0.0	0.0	7.00	7.00	0	434	92
0.1	$3.47x10^{-3}$	6.54	6.81	$1.38x10^{-3}$	603	147
0.2	$7.87x10^{-3}$	6.28	6.63	$2.56x10^{-3}$	747	194
0.3	$1.26x10^{-2}$	6.10	6.50	$3.55x10^{-3}$	867	234
0.4	$1.74x10^{-2}$	5.98	6.41	$4.31x10^{-3}$	960	264
0.5	$2.21x10^{-2}$	5.88	6.34	$4.99x10^{-3}$	1043	291
0.6	$2.68x10^{-2}$	5.80	6.28	$5.62x10^{-3}$	1120	316
0.7	$3.16x10^{-2}$	5.74	6.23	$6.21x10^{-3}$	1190	340
0.8	$3.63x10^{-2}$	5.68	6.19	$6.75x10^{-3}$	1257	361
0.9	$4.10x10^{-2}$	5.63	6.15	$7.26x10^{-3}$	1319	381
1.0	$4.60x10^{-2}$	5.58	6.12	$7.74x10^{-3}$	1377	400
1.1	$5.04x10^{-2}$	5.54	6.09	$8.19x10^{-3}$	1432	418

for these simulations was greater than the pH for the simulations that did not equilibrate with calcite, which was expected. However, the modeled pH, alkalinity, and calcium concentration were all greater than observed values during the injection of CO_2. Therefore, because the observed pH was between the two modeled pH values, it is evident that some calcite dissolved, but not enough to reach saturation. This is likely because the fast groundwater velocity (3 m/d) replaces the pore water before saturation with respect to calcite is reached.

A final SOLMINEQ simulation was performed to determine the approximate concentration of calcite dissolving with high P_{CO2} in the aquifer. For this, the P_{CO2} was held constant while the amount of calcite dissolved was varied. The results of the modeling along with observed data are shown in Figure 13. The water samples taken before the injection started (background) have higher pH and lower alkalinities than samples taken during the CO_2 injection, which was expected. SOLMINEQ estimated the background P_{CO2} to be less than 0.05 bars. Upon the addition of CO_2, the pH decreased. This change in pH enhanced dissolution of carbonates and increased the alkalinity of the groundwater. Isobars of P_{CO2} are shown as solid lines in the graph, and specific concentrations of calcite dissolved are shown with dashed lines. The P_{CO2} isobars start at a dissolved calcite concentration of 0 moles/kg of water, and end at complete calcite saturation, which varies depending on P_{CO2}. Greater P_{CO2} can cause more calcite to dissolve. A majority of the groundwater samples fall within a P_{CO2} range of 0.8 to 1.1 bar and a dissolved calcite concentration range of $3x10^{-3}$ to $6x10^{-3}$ moles/kg of water. The outlier was a sample taken shortly after CO_2 injection started. Therefore, it had not

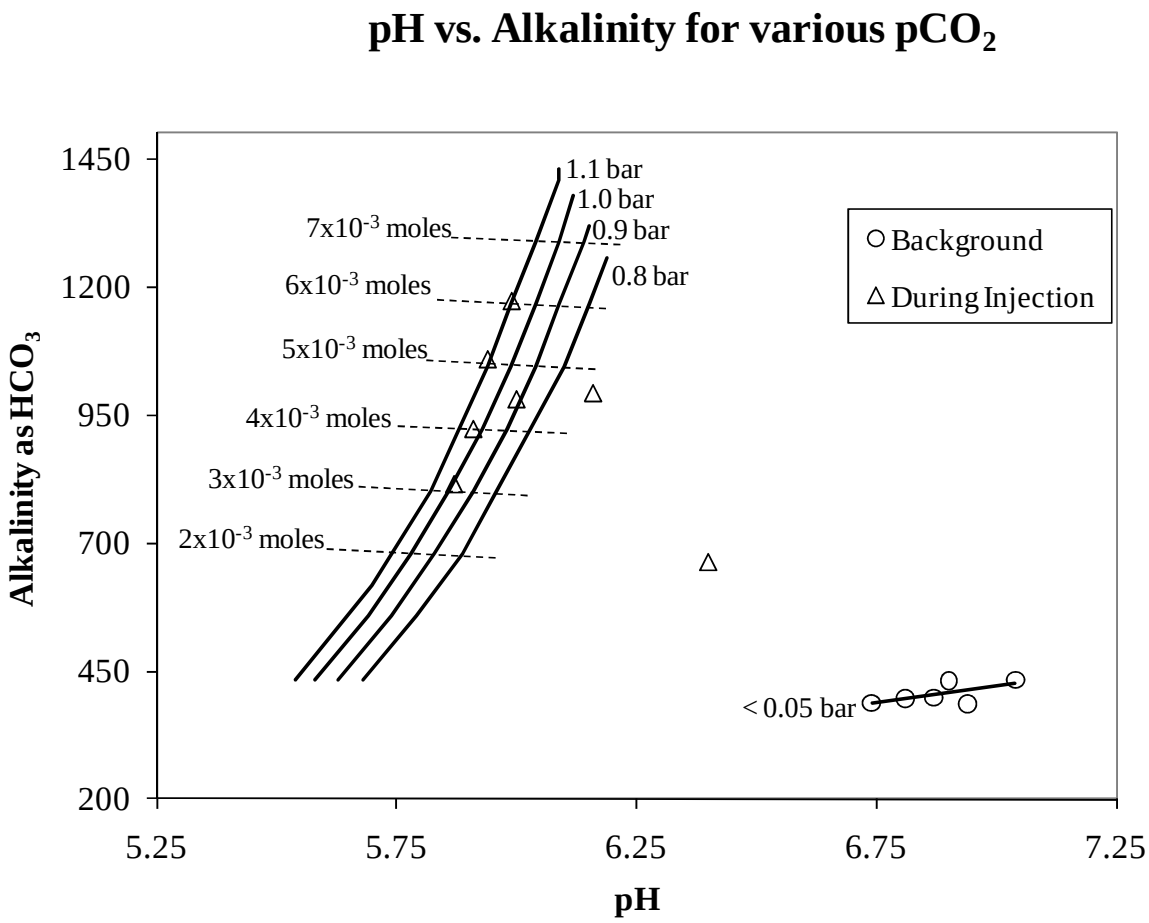

Figure 13. SOLMINEQ modeling results compared with observed water chemistry data for the dissolution of various concentrations of calcite (moles/kg water) with constant P_{CO2} (bars). The amount of calcite dissolution ranges from 0 moles/kg water to the maximum amount needed to reach calcite saturation for each of four P_{CO2} values. The amount of dissolved calcite is shown with dashed lines, and isobars are shown with solid lines. Finally, observed pH and alkalinity data are shown in circles (background water samples from 2008, Table 21) and triangles (water samples collected during CO_2 injection in 2008, Table 22).

been exposed to maximum amounts of P_{CO2} at the time of sampling. However, for all of these models, dissolving only calcite overestimated the calcium concentration and underestimated the magnesium concentrations. Therefore, it is likely that the calcite in the aquifer is high magnesium, but not high enough to be dolomite.

With geochemical modeling, it was apparent that increases in P_{CO2} decreases the saturation index of calcite and other carbonate minerals. Furthermore, without the dissolution of calcite, the pH would have been lower than observed values. On the other hand, modeling complete saturation of calcite with increased P_{CO2} overestimated the changes in pH, alkalinity, and calcium in the water compared to observed values. Therefore, it is likely that calcite did not dissolve to saturation, which is shown through the PHREEQC modeling. It is likely that the fast groundwater flow replaced pore waters before they were saturated with respect to calcite.

It is important to mention that calcite dissolution is not the only geochemical process that responds to decreased pH. Ion exchange on organic and inorganic surfaces, especially of alkali and alkaline earth elements, is also affected by pH (Krauskopf and Bird, 1995).

Groundwater Chemistry Compared with Mineral Chemistry

Thus far, it has been shown with groundwater modeling and sequential extractions that most of the geochemical changes in the groundwater are due to dissolution of carbonates and ion exchange. Dissolution of trace amounts of manganese oxides during CO_2 injection is also possible, but it would have a smaller effect on the groundwater chemistry. It is possible that as minerals dissolve, their cation ratios are preserved in the groundwater. Therefore, molar ratios of elements in the groundwater and the sediment were compared and the results are shown in Table 25.

Table 25. Concentration ranges and molar ratios of calcium and manganese compared with elements that showed similar ratios in groundwater and the sequential extraction.

	Concentration Range in the Groundwater	Molar Ratios in the Groundwater	Concentration Range in the Sequential Extraction of the Sediment	Molar Ratios in the Sequential Extraction of the Sediment
Calcium	83.8 - 204 mg/L			
Magnesium	16.4 - 69.9 mg/L	4.03×10^{-1}	11.5 - 38.2 mg/L	3.65×10^{-1} (A)[†]
Strontium	0.2 - 0.8 mg/L	1.45×10^{-3}	0.3 - 1.1 mg/L	2.36×10^{-3} (A)
Barium	0.1 - 0.3 mg/L	3.25×10^{-4}	1.0 - 3.1 mg/L	4.41×10^{-4} (B)
Uranium	3.5 - 6.2 µg/L	7.86×10^{-7}	0.7 - 5.9 ug/L	5.12×10^{-7} (B)
Manganese	< 0.1 - 0.3 mg/L			
Cobalt	0.2 - 3.1 ug/L	5.80×10^{-3}	0.5 - 9.6 ug/L	8.22×10^{-3} (C)

[†]Extraction Step for which molar ratio was calculated.

The molar ratios were taken as the slope of a linear regression through the concentration data of the elements in the comparison. There were only a few molar ratios that showed agreement between the groundwater and the sediment. Magnesium to calcium, and strontium to calcium ratios strongly resembled the ratios seen in the ion exchange extraction (Step A), but not in the carbonate extraction (Step B, not shown). For every mole of magnesium, there were approximately 2.5 moles of calcium in both the groundwater and ion exchange phase of the sequential extraction. Likewise, the strontium to calcium molar ratio is similar for both the groundwater and ion exchange phase of the extraction. For every mole of strontium in the groundwater or Step A of the sequential extraction, there were approximately 500 moles of calcium. The similar molar ratios in the groundwater and ion exchange extraction results indicate that there was some ion exchange occurring in the aquifer. This is reasonable because the pH of the groundwater decreased with the addition of CO_2, and pH strongly affects ion

exchange of alkali and alkaline earth elements. According to Carroll (1959), at low pH hydrogen ions are free to exchange with other cations. Thus, cations that were once bound to the sediment are free in the groundwater.

Calcium was also related to barium and uranium in both the groundwater and the carbonate phase (Step B) of the sequential extraction. However, Ba and U were also related to manganese oxide dissolution. Geochemical modeling showed that manganese oxide dissolution is less common, so it is likely that dissolution of calcite in the sequential extraction and the groundwater led to these similarities. Furthermore, the ratios of calcium to barium and uranium in Step B of the sequential extraction are similar to those found in the groundwater with the injection of CO_2. For every mole of barium in the groundwater or carbonate phase of the sequential extraction, there were approximately 260 moles of calcium. Likewise for uranium; for every mole of uranium, there were approximately $1.5x10^6$ moles of calcium. As shown with geochemical modeling, carbonate dissolution occurred in the aquifer with the addition of CO_2, so these results are reasonable.

Manganese and cobalt have similar molar ratios in both the groundwater and the manganese oxide dissolution step of the sequential extraction. This may reflect dissolution of small amounts of manganese oxides in the sediment with the injection of CO_2, which is evidenced by the undersaturation of hausmannite shown in Table 23. Even though hausmannite does not occur in large quantities in alluvial settings, trace amounts of the mineral or a similar manganese oxide may account for increases in manganese in the groundwater during CO_2 injection. Other metals may have been liberated with

manganese oxide dissolution, but cobalt can be uniquely associated with replacement of manganese cations in the lattice of manganese oxide crystals (McKenzie, 1972).

Dissolved organic matter in the ZERT groundwater did not change with the addition of CO_2 (Kharaka et al., 2010). Thus, it is inferred that organic molecular structures were unaffected by the pH change in the aquifer, and cations incorporated into these molecular structures were also unaffected. However, organic matter is also capable of ion exchange. For alkali and alkaline earth elements, ion exchange is sensitive to pH (Krauskopf and Bird, 1995). Thus, if ion exchange was occurring on organic surfaces, it was likely occurring during Step A. Step E was destructive and released elements that were bound to organic compounds in any way.

Trace metal concentrations, in general, increased in the groundwater with the addition of CO_2 (tables 21 and 22). However, important trace metals including copper, zinc, chromium, and lead were not detected in extraction step A. The lack of trace metals in Step A is most likely due to the strong dilution factor that was required for ICP-MS analysis, as discussed in the results section. It is likely there were trace metals involved in ion exchange in both the sequential extraction and aquifer; however, the specific elements and quantities remain unknown. Furthermore, these trace metals were released in steps C and E, and with the exception of zinc, Step B. Due to the multiple sources of these elements, it is difficult to pinpoint the primary mechanism responsible for their release in the groundwater with the CO_2 injection.

The sequential extraction had sediment to reagent ratios of around 1:10 by volume. The procedure produced concentrations of ions equivalent to or greater than that

found in the groundwater during the CO_2 injection (see Table 25 for some elements in extraction Steps A, B, and C). However, the aquifer has a porosity from 23 to 28% (unpublished data), which means the sediment to groundwater ratio is approximately 3:1. Therefore, the sediment is able to provide more than enough elements to account for the increases seen in the groundwater during the CO_2 injection even with the high groundwater velocity.

Soil type was not an immediate factor contributing to the water-rock-gas interactions in the aquifer. As mentioned before, the groundwater resides approximately 1 m below the ground surface during the summer. From an average of 8 core samples, the topsoil is 42 cm thick, and the B horizon is 32 cm thick. Together, these two soil layers comprise the top 74 cm of soil, which is tens of centimeters above the 1-m water table. Thus, there is an unsaturated depth of a few tens of centimeters within the sandy gravel aquifer. Therefore, it can be inferred that the topsoil and B horizon did not have an immediate impact on the groundwater geochemistry during times when there was no recharge of meteoric water. The lithic fragments and secondary minerals within the sandy gravel provided adequate amounts of exchange sites, and of carbonate and oxide minerals; however, the low concentration of organic matter may have excluded organics from contributing metals or other elements to the groundwater.

More data and research are required to determine the release mechanisms for other metals into the groundwater during CO_2 injection. The sequential extraction provides useful information regarding which elements were associated with certain phases; however, many elements such as calcium, magnesium, manganese, copper, zinc,

and lead were present in many sources that may be affected by CO_2. For instance, lead was common in several phases in the sediment including manganese oxides and organic matter. Slight decreases in pH affected the lead in both of these phases, and a simple molar ratio was inadequate for distinguishing its true source.

Furthermore, the sequential extraction reagents, especially for steps A and B, were too concentrated for the analytical method. To be analyzed with ICP-MS, the supernatants had to be diluted to a higher degree than supernatants from other extraction steps, which forfeited sensitivity of detection of trace elements. This is a great loss when trying to determine the sources of metals in the sediment, because it represents a hole in the data set. It is possible that reagents of a lesser concentration, which would require less dilution for analysis, would be adequate for the sequential reactions. Another possible solution to this problem is to analyze the supernatants with another technique, such as atomic absorption spectroscopy (AAS), which only tests for one element at a time, or to subject aquifer material to Micro-XRF, which can pinpoint element locations on a crystal surface. Both of these are more time consuming and costly than the approach that has been presented here, not to mention that ICP-MS can detect very small quantities of an element. However, other methods have the potential to add more detailed information to determining the exact sources of elements in aquifer material.

Finally, a more detailed geochemical model incorporating mineral phases and associated trace elements would be a useful tool for determining release mechanisms of cations into the groundwater with the addition of CO_2. This is beyond the scope of this project and the simple geochemical modeling presented here.

CONCLUSIONS

The sequential extraction procedure provided valuable information pertaining to cation concentrations associated with exchange reactions, and with carbonate, oxide, sulfide, and organic phases in the soil. Topsoil, carbonate-rich B horizon samples, and sandy gravel aquifer material were digested to determine the abundant minerals and their associated trace metals. The results showed many expected ion relationships such as calcium and magnesium associated with carbonate phases, and several trace metals associated with iron and manganese oxides.

Geochemical modeling of the groundwater revealed that, with the addition of carbon dioxide, saturation indices of many carbonates and a few manganese oxides decreased while those of most other crystalline oxides increased. This indicated that groundwater was becoming more undersaturated with respect to carbonate minerals and some manganese oxides, thus these minerals are more likely to dissolve with the addition of CO_2. Further geochemical modeling showed that, with the addition of CO_2, the pH of the system would drop below observed values unless carbonates were dissolving; however, carbonates were not dissolving to saturation. It is likely that only a few moles of calcite per kilogram of water were dissolving in the system, which is attributed to the quick groundwater flow in the aquifer. Sequential extraction data revealed that carbonate minerals are associated with high concentrations of calcium and magnesium, as well as barium and uranium.

With the increase of cations in the groundwater from calcite dissolution and the decrease in pH of the system due to an increase in carbon dioxide, it can be inferred that ion exchange of alkali and alkaline earth metals also occurred. Literature shows that exchange of these cations is sensitive to pH. It is difficult to distinguish ion exchange on organic and inorganic surfaces. Organic molecules are able to exchange cations and incorporate them into their molecular structures. Also, low concentrations of organic matter in the sandy gravel, the aquifer material most affected by CO_2, limited the impact organics have on the groundwater chemistry. Since dissolved organic matter in the groundwater did not change with the release of carbon dioxide, it was assumed that cations incorporated into the organic structure are unaffected while ion exchange on organic surfaces was active.

APPENDIX A. ZERT CORE LOGS

Sediment cores were collected from the ZERT field site December 2008. The wells were drilled with a Geoprobe rig, which uses pneumatic action to punch through the earth. The cores were drilled in three sections, typically four feet at a time. Both the topsoil and B horizon sediment are coherent, thus the recovery of these sections was quite good. However, due to the loose nature of the unconsolidated sandy gravel aquifer, core recovery in deeper sections was poor.

The cores were frozen and transported with dry ice to the USGS laboratory in Menlo Park, CA. Here, they were stored in a freezer until logged and sampled. If a section of core is denoted as frozen in the log, it means the core had not thawed completely when logged. It was important to note because frozen core may have a different color than thawed or dry core.

Table A1. W6 core log.

Theoretical Depth (ft)	Recovered Depth (cm)	Description
0-3.5'	0-5cm	grass and air
	5-30cm	dark brown, clay rich, plastic soil with roots througout. Slightly fizzes with acid large rock most likely broken by geoprobe
	30-39cm	plastic clay grading from dk brown to lt brown indicating a gradation into caliche
	39-57cm	10YR 5/4. Caliche zone. Highly reactive with HCl, very fine grained and plastic with some roots. Few larger, rounded grains between 1-3cm.
	57-64cm	Sandy gravels (with some caliche smearing on kevlar sleeve).
3.5-8'	0-15cm	Slough with a large grain cored through by the geoprobe at 11-15cm.
	15-75.5cm	10YR 3/3 dark brown. Coarse sandy gravel, possibly higher percentage of gravels than other cores. Grains as large as 4cm. Gravels appear to have been rounded then broken, possible geoprobe damage? Saturated below 30cm (from top of 4-8' core?). Lightly fizzes with acid throughout the core.
8-10'	0-41cm	10YR 3/3 dark brown. Coarse sandy gravel, few fines. Grains up to 4cm, possibly damaged by geoprobe. Some plastic from a broken core catcher is present. Few orange clay streaks near 37cm.

Table A2. W7 core log.

Theoretical Depth (ft)	Recovered Depth (cm)	Description
0-4'	0-26	10YR 2/2 yellowish dark brown (frozen), clay/organic-rich topsoil. Fine grained with roots. 4 in. (10.2 cm) removed from top of core in the field.
	26-70	10YR 5/4 yellowish brown (frozen). Caliche. Very fine grained, matrix supported, and plastic zone. Containing some sand and gravel. Fizzes vigorously with acid.
	70-86.5	Dark Brown (frozen). Coarse sandy gravel. Few fines. Wet but not saturated. Possible large, broken up carbonate grain.
4-8'	0-64.5	Color grades from 5YR3/2 (dark reddish brown) at the top of the core to 5YR 4/6 (yellowish red) at the bottom of the core (frozen). Coarse sandy gravel. Large grains are rounded, though some are seemingly freshly broken. Fines are subrounded to subangular. Core is mostly saturated. Very small white grains fizz with acid throughout the core.
8-10'	0-40	Brown (frozen). Saturated. Coarse sandy gravel, few fines. Rounded pebbles and cobbles up to the width of the core (4cm).

Table A3. W8 core log.

Theoretical Depth (ft)	Recovered Depth (cm)	Description
0-4'	0-45	10YR 3/3 dark brown, very fine grained, clayey-plastic soil with a few large (>2cm) pebbles. Roots run throughout the core.
	45-63	10YR 4/3 brown soil, clayey and plastic with few small (~1cm) rounded pebbles. Roots run throughout, and the soil fizzes with acid.
	63-72	A continuation of the caliche zone described between 45-63cm
	72-85	Coarse gravelly sand with grains up to 3cm. Little clay. 10YR3/3 dark brown. Sand grains= subangular-subrounded, gravels =
4-8'	0-52	Moderately well sorted coarse sand, fine gravel with little clay. Grains are subrounded to rounded. 10YR3/3 dark brown.
	52-64	Saturated conditions appear to begin at 52cm with possibility of an increase in clay content
8-10'	0-38	10YR 3/3 dark brown. Coarse sand/fine gravel moderately well sorted material with little clay. Grains are as large as 4cm. Larger grains are well rounded, smaller grains are subangular to subrounded.

REFERENCES CITED

Albering, J.H., 1999, Structural chemistry of manganese dioxide and related compounds, *in* Besenhard J.O., ed., Handbook of Battery Minerals: New York, Wiley-VHC, p. 85-110.

Carroll, D., 1959, Ion exchange in clays and other minerals: GSA Bulletin, v. 70, p. 749-780.

Chao, T.T., 1984, Use of partial dissolution techniques in geochemical exploration: Journal of Geochemical Exploration, v. 20, p. 101-135.

Chao, T.T., and Theobald, P.K., 1976, The significance of secondary iron and manganese oxides in geochemical exploration: Economic Geology, v. 71, p. 1560-1569.

Deer, W.A., Howie, R.A., and Zussman, J., 1978, An Introduction to the Rock-Forming Minerals: London, Longman Group, 528 p.

Deutsch, W.J., 1997, Groundwater Geochemistry: Fundamentals and Applications to Contamination: Boca Raton, CRC Press, 221p.

Hall, G.E.M, Vaive, J.E., Beer, R., and Hoashi, M., 1996, Selective leaches revisited, with emphasis on the amorphous Fe oxyhydroxide phase extraction: Journal of Geochemical Exploration, v. 56, p. 59 – 78.

Hall, G.E.M., 1998, Analytical perspective on trace element species of interest in exploration: Journal of Geochemical Exploration, v. 61, p. 1-19.

Hewett, D.F., 1972, Manganite, hausmannite, braunite: features and modes of origin: Economic Geology, v. 67, p. 83-102.

Holloway, S., 2005, Underground sequestration of carbon dioxide – a viable greenhouse gas mitigation option: Energy, v. 30, p. 2318-2333.

Intergovernmental Panel on Climate Change (IPCC), 2005, Special report on carbon dioxide capture and storage: Cambridge University Press: http://www.ipcc-wg3.de/activity/special-reports/.files-images/SRCCS-TechnicalSummary.pdf (accessed September 17, 2009).

Jackson, M.L., 1958, Soil Chemical Analysis: London, Prentice Hall, 498p.

Kennedy, V.H., Sanchez, A.L., Oughton, D.H., and Rowland, A.P., 1997, Use of single and sequential chemical extractants to assess radionuclide and heavy metal availability from soils for root uptake: Analyst, v. 122, p. 89R-100R.

Kharaka, Y.K., Gunter, W.D., Aggarwal, P.K., Perkins, E.H., and DeBraal, J.D., 1988, Solmineq 88: A computer program for geochemical modeling of water-rock interactions: U.S.G.S. Water-Resources Investigation Report 88-4227, 420 p.

Kharaka, Y.K., Thordsen, J.J., Kakouros, E., Ambats, G., Herkelrath, W.N., Beers, S.R., Birkholzer, J.T., Apps, J.A., Spycher, N.F., Zheng, L., Trautz, R.C., Rauch, H.W., and Gullickson, K.S., 2010, Changes in the chemistry of shallow groundwater related to the 2008 injection of CO_2 at the ZERT field site, Bozeman, Montana: Environmental Earth Sciences, v. 60, p. 273-284.

Klein, C., 2002, The 22nd Edition of the Manual of Mineral Science: New York, John Wiley and Sons, Inc., 641p.

Krauskopf, K.B., and Bird, D.K., 1995, Introduction to Geochemistry, 3 ed: San Francisco, WCB/McGraw-Hill, 647p.

Lonn, J.D., and English, A.R., 2002, Prelimiary geologic map of the eastern part of the Gallatin valley, Montana: Montana Bureau of Mines and Geology Open File Report 457.

Maher, W.A., 1984, Evaluation of a sequential extraction scheme to study associations of trace elements in estuarine and oceanic sediments: Bulletin of Environmental Contamination and Toxicology, v. 32, p. 339-344.

Malcolm, R.L., and Kennedy, V.C., 1970, Variation of cation exchange capacity and rate with particle size in stream sediment: Water Pollution Control Federation Journal, v. 42, p. R153-R160.

Mayo, J.T., Yavuz, C., Yean, S., Cong, L., Shipley, H., Yu, H., Falkner, J., Kan, A., Tomson, M., and Colvin, V.L., 2007, The effect of nanocrystalline magnetite size on arsenic removal: Science and Technology of Advanced Materials, v. 871, p 71-75: http://www.iop.org/EJ/abstract/1468-6996/8/1-2/A13/ (accessed March 23, 2011).

McKenzie, R.M., 1972, The sorption of some heavy metals by the lower oxides of manganese: Geoderma, v. 8, p. 29-35.

Modak, D.P., Singh, K.P., Chandra, H., and Ray, P.K., 1992, Mobile and bound forms of trace metals in sediments of the Lower Ganges: Water Resources, v. 26, p. 1541-1548.

Papp, C.S.E., Filipek, L.H., and Smith, K.S., 1991, Selectivity and effectiveness of extractants used to release metals associated with organic matter: Applied Geochemistry, v. 6, p. 349-353.

Parkhurst, D.L., and Appelo, C.A.J., 1999, User's guide to PHREEQC (version 2) – a computer program for speciation, reaction-path, 1D-transport, and inverse geochemical calculations: U.S. Geological Survey Water Resources Investigation Report 99-4259, 312p: http://wwwbrr.cr.usgs.gov/projects/GWC_coupled /phreeqc/html/final.html (accessed 2/13/2011).

Rashid, M.A., 1974, Absorption of metals on sedimentary and peat humic acids: Chemosphere, v. 13, p. 115-123.

Reardon, E.J., Dance, J.T., and Lolcama, J.L., 1983, Field determination of cation exchange properties for calcareous sand: Ground Water, v. 21, p. 421-428.

Span, D., and Gaillard, J-F., 1986, An investigation of a procedure for determining carbonate-bound trace metals: Chemical Geology, v. 56, p. 135-141.

Spangler, L.H., Dobeck, L.M., Repasky, K., Nehrir, A., Humphries, S., Barr, J., Keith, C., Shaw, J., Rouse, J., Cunningham, A., Benson, S., Oldenburg, C.M., Lewicki, J.L., Wells, A., Diehl, R., Strazisar, B., Fessenden, J., Rhan, T., Amonette, J., Barr, J., Pickles, W., Jacobson, J., Silver, E., Male, E., Rauch, H., Gullickson, K., Trautz, R., Kharaka, Y., Birkolzer, J., and Wielopolski, L., 2009, A controlled field pilot for testing near surface CO_2 detection techniques and transport models: Energy Procedia, v. 1, p. 2143-2150.

Schnitzer, M., 1978, Humic substances: chemistry and reactions, *in* Schnitzer, M., and Khan, S.U., eds., Developments in Soil Science 8 – Soil Organic Matter: New York, Elsevier North-Holland Inc., p. 1-58.

Szalay, A., 1964, Cation exchange properties of humic acids and their importance in the geochemical enrichment of UO_2^{++} and other cations: Geochimica et Cosmochimica Acta, v. 28, p. 1605-1614.

Tessier, A., Campbell, P.G.C., and Bisson, M., 1979, Sequential extraction procedure for the speciation of particulate trace metals: Analytical Chemistry, v. 51, p. 844-851.

U.S. Environmental Protection Agency (EPA), 2001, Methods for collection, storage, and manipulation of sediments for chemical and toxicological analyses: Technical Manual EPA-823-B-01-002, 208p.: http://nepis.epa.gov/EPA/html/DLwait.htm ?url=/Adobe/PDF/20003PLT.PDF (accessed April 6, 2011).

U.S. Environmental Protection Agency (EPA), 2009, National Primary Drinking Water Regulations: <http://www.epa.gov/safewater/consumer/pdf/mcl.pdf> (accessed September 18, 2009).

Vuke, S.M., Lonn, J.D., Berg, R.B., and Kellogg, K.S., 2002, Preliminary geologic map of the Bozeman 30' x 60' Quadrangle, southwestern Montana: Montana Bureau of Mines and Geology Open File No. 469, scale 1:100,000. <http://www.mbmg.mtech.edu/ pdf_100k/bozeman-tiled.pdf> (accessed May 19, 2011).